Received: 19 September 2019 | Revised: 3 January 2020 | Accepted: 4 January 2020

DOI: 10.1002/wcms.1463

ADVANCED REVIEW

WIREs COMPUTATIONAL MOLECULAR SCIENCE WILEY

Coupled cluster theory in the condensed phase within the singles-T density scheme for the environment response

Marco Caricato

Department of Chemistry, University of Kansas, Lawrence, Kansas

Correspondence
Marco Caricato, Department of Chemistry, University of Kansas, 1567 Irving Hill Rd, Lawrence, KS 66045.
Email: mcaricato@ku.edu

Funding information
Division of Chemistry, Grant/Award Number: CHE-1650942

Abstract

Reliable simulations of molecules in condensed phase require the combination of an accurate quantum mechanical method for the core region, and a realistic model to describe the interaction with the environment. Additionally, this combination should not significantly increase the computational cost of the calculation compared to the corresponding in vacuo case. In this review, we describe the combination of methods based on coupled cluster (CC) theory with polarizable classical models for the environment. We use the polarizable continuum model (PCM) of solvation to discuss the equations, but we also show how the same theoretical framework can be extended to polarizable force fields. The theory is developed within the perturbation theory energy and singles-T density (PTES) scheme, where the environmental response is computed with the CC single excitation amplitudes as an approximation for the full one-particle reduced density. The CC-PTES combination provides the best compromise between accuracy and computational effort for CC calculations in condensed phase, because it includes the response of the environment to the correlation density at the same computational cost of in vacuo CC. We discuss a number of numerical applications for ground and excited state properties, based on the implementation of CC-PTES with single and double excitations (CCSD-PTES), which show the reliability and computational efficiency of the method in reproducing experimental or full-CC data.

This article is characterized under:
Electronic Structure Theory > Ab Initio Electronic Structure Methods
Electronic Structure Theory > Combined QM/MM Methods
Software > Quantum Chemistry

KEYWORDS

coupled cluster, condensed phase, response properties, polarizable embedding

1 | INTRODUCTION

Most phenomena of interest in chemistry occur in condensed phase. Thus, accounting for environmental effects in quantum chemistry calculations is often essential to obtain a correct description of a particular process. Unfortunately, the quantum mechanical (QM) treatment of the environment is not possible in the vast majority of cases, due to the computational scaling of even the simplest of QM approaches. Therefore, hybrid or focused models are employed,

where the core region is treated at a QM level, and the environments is described in a simplified manner, often based on some classical physics model.[1–5] In this way, although an accurate description of the entire system is sacrificed, the interaction with the core region, where the process of interest occurs, includes the right physics. These classical models can be based on an atomistic representation of the environment, for instance with a molecular mechanics (MM) force field,[1–3] or on continuum models, where the environment is represented by a polarizable medium characterized by some macroscopic quantity, for example, the electric permittivity.[4,5] Explicit models are obviously more realistic, but they also require a considerable computational effort to obtain a proper averaging of the possible configurations of the particles surrounding the core region. MM force fields may be based on a series of fixed atomic charges, or they can include a polarizable component for the mutual polarization with the core region. In the latter case, the description of the interaction with the environment is even more realistic, but the computational effort is further increased. On the other hand, continuum (or implicit) models cannot describe direct core-environment interactions, but they account for bulk effects and mutual polarization with the core region very efficiently, because the conformational sampling is implicit in the medium's permittivity.[6] The choice of which model to employ depends on the application of interest and on the available computational power.

Although the environment is important to obtain a realistic representation of the experimental settings, treating the core region with an accurate level of theory is fundamental for reliable simulations. In this respect, coupled cluster (CC) theory plays a leading role in quantum chemistry for the study of molecular ground and excited states as well as response properties.[7,8] The appeal of the theory is that, in principle, the exact form of the wave function is known (within the nonrelativistic, Born–Oppenheimer framework). Although evaluating the exact wave function and energy is practically seldom possible, there is a well defined way to write approximate versions of the theory, and a clear path to systematically improve the description of the system. This is contrary to modern density functional theory (DFT), where the form of the exact functional is not known, and progress towards the exact density representation is not straightforward. In practice, DFT still constitutes the workhorse of quantum chemistry simulations, but CC methods are used when a high level of accuracy and reliability is necessary. Therefore, extending the ability of CC methods to include the effect of the environment is highly desirable.

The combination of electron correlation methods with continuum models dates back to the early 1990s, with the work of Olivares del Valle and Tomasi on perturbation theory (PT) and the polarizable continuum model of solvation (PCM).[4,5,9,10] In these papers, the solvent response was included explicitly in the reference Hartree–Fock (HF) equations as well as in the PT equations. Therefore, the solvation scheme was called PT energy and density (PTED), since it involved the correlation density. The approximation where the solvent response was only included in the HF equations was called PTE, as the correlation density is not necessary. The PTED scheme requires a PCM macro-iteration procedure to reach mutual polarization between the solute and the solvent. Thus, it is considerably more computationally demanding than the corresponding in vacuo PT and PCM-PTE approaches, which do not require the correlation density and the macro-iteration procedure. We will use the PTED and PTE designation also for the combination of CC theory and PCM, because the basic derivation is similar.

The first implementation of CC theory with a continuum solvation model was presented by Christiansen and Mikkelsen (CM).[11,12] Although their solvation model was not as flexible and elaborate as PCM, the theory for the interfacing with CC methods is essentially the same as the PTED scheme. The main difference of the CM approach compared to the initial PTED scheme in References 9, 10 is that in the former the HF calculation is performed in vacuo, and the solute-solvent interaction is accounted for entirely in the CC equations. This choice has two disadvantages in practical calculations with truncated CC wave functions: (a) most of the solvent response is due to the polarization of the HF orbitals, which cannot be recovered by the CC single excitation amplitudes alone, (b) the PTE approximation cannot be invoked. Nevertheless, CM also developed the theory for electronic excitations and response properties through response theory, which extended the use of the method to study photochemistry and other interactions with external fields.[11–13] Later on, this theoretical framework was utilized by Kongsted and coworkers to combine CC theory with a polarizable force field based on an induced multipole model.[14–25] The theory for the combination of CC methods and PCM with the PTED and PTE schemes was presented by Cammi, who described the extension to excited state phenomena using the linear response (LR) formalism as well as the state specific formalism (SS).[26–28] Cammi also collaborated with Ehara and co-workers to combine PCM with the symmetry adapted cluster-configuration interaction (SAC-CI) method,[29–33] which is closely related to CC theory. It is also important to mention the combination of CC methods with other embedding schemes, albeit only at the PTE level.[34–41]

Our contributions to this field come from the first implementation of the PCM-PTED scheme with CC with single and double excitations (CCSD-PCM-PTED) for ground and excited state properties, and from the definition of a new

coupling scheme, intermediate between PTED and PTE, to maintain the cost of CC-PCM calculations virtually identical to that of in vacuo CC.[42–54] In fact, the main scope of this review is to discuss this new scheme, which we call "singles-T density" approximation for the correlation solvent response, or PTES. The PTES scheme includes the correlation solvent response explicitly, which is fundamental for a qualitatively correct description of the process of interest, but it avoids the PCM macro-iteration procedure that makes the PTED scheme so computationally demanding. The expression "singles-T" approximation for the environment is used because the ground state solvent response can be evaluated by using just the CC single excitation amplitudes. However, it is important to emphasize that "singles" here is not related to the level of truncation of the CC expansion. Indeed, we discuss the equations in a general form, without invoking any truncation of the CC wave function ansatz, even if in practice we implemented the method for CCSD-PCM. This body of work includes ground and excited state energy and energy gradients with the SS and LR formalisms.[44–50,52,54] Additionally, we discuss how this theoretical framework can be extended to polarizable MM force fields with minimal effort.[53]

The review is organized as follows: Section 2 presents in detail the theory for ground and excited state CC-PCM-PTES, and how the same theoretical framework can be easily extended to polarizable MM force fields; Section 3 describes a series of applications of the CCSD-PCM schemes, and compares the accuracy with respect to experiment, and the computational cost with respect to in vacuo CC; finally, Section 4 contains an overall discussion and concluding remarks.

2 | THEORY

In this section, we present a review of the theory and of the implementation details for the CCSD-PCM-PTES method for ground and excited states. However, it is useful to introduce first the notation that we will utilize for the remaining of the paper. The coupled cluster ground state excitation operators $\hat{T}$, and the auxiliary deexcitation operators $\hat{\Lambda}$, are defined as[7,8]:

$$\begin{aligned} \hat{T} &= \sum_{n=1}^{N_{el}} \hat{T}_n = \sum_{n=1}^{N_{el}} t_n \hat{\tau}_n \\ \hat{\Lambda} &= \sum_{n=1}^{N_{el}} \hat{\Lambda}_n = \sum_{n=1}^{N_{el}} \lambda_n \hat{\tau}_n^\dagger \end{aligned} \tag{1}$$

where N_{el} is the number of electrons, and $\hat{\tau}_n$ is an elementary excitation operator; n collectively represents the level of excitation/deexcitation, for example, $\hat{\tau}_1$ indicates all one-electron excitations from the reference wave function Φ^0:

$$\hat{\tau}_1 \,|\, \Phi^0\rangle = |\, \Phi^1\rangle. \tag{2}$$

Similarly, $\hat{\tau}_n^\dagger$ is an elementary deexcitation operator. The amplitudes t_n (and λ_n) indicate the weight of any particular excitation in the CC exponential ansatz:

$$|\, \Phi_0^{CC}\rangle = e^{\hat{T}} \,|\, \Phi^0\rangle \tag{3}$$

In Equation 3 and in the following, we use the n numerical superscript to indicate n-th excited Slater determinants, and a numerical subscript to index the electronic state. It is also convenient to introduce a short-hand notation for normal-ordered, similarity transformed operators[7,8]:

$$\bar{X}_N = e^{-\hat{T}} \hat{X} e^{\hat{T}} - \langle X^0 \rangle \tag{4}$$

where the last term on the right-hand side is the expectation value of the operator $\hat{X}$ computed with the reference wave function. When convenient, we will also use the following short-hand notation for the bra function:

$$\langle \Lambda | = \langle \Phi^0 | \left(\hat{1} + \hat{\Lambda} \right) \tag{5}$$

where $\hat{1}$ is a unit operator that leaves the function unchanged. Note that the deexcitation operator $\hat{\Lambda}$ performs as an excitation operator when it operates on the left.

The PCM charges $\mathbf{Q}$ are computed by solving a linear system of the form[4,5]:

$$\mathbf{Y}(\{R_{cav}\}, \varepsilon)\mathbf{Q}(\gamma) = -\mathbf{V}(\gamma) \tag{6}$$

where $\mathbf{Y}(\{R_{cav}\}, \varepsilon)$ is the PCM interaction matrix, whose specific form changes with the flavor of PCM, but that in general depends on the shape of the solute cavity (determined by the atom-centered cavity radii $\{R_{cav}\}$) and the dielectric permittivity ε. The term $\mathbf{V}(\gamma)$ on the right-hand side is the electrostatic potential generated by the solute nuclei and electrons on the cavity surface. Thus, both $\mathbf{V}$ and $\mathbf{Q}$ depend explicitly on the solute one-particle electron density γ. The expression in Equation 6 already assumes that the integration over the cavity surface is performed approximately as a sum over finite elements. The various formulations of the PCM equations, and of the cavity shape and its discretization are discussed in detail elsewhere.[4,5,55] A key point for the following discussion is that we assume that the matrix $\mathbf{Y}(\{R_{cav}\}, \varepsilon)$ is symmetric, which limits the current implementation of CC-PCM methods to the conductor-like formulation (CPCM)[56,57] and the symmetric version of the integral equation formalism PCM (IEFPCM).[58]

2.1 | Ground state

The electronic energy expression for the solute in the CC-PCM-PTED method can be expressed in terms of a Lagrangian[26]:

$$\begin{aligned} G_0 = &\ \langle \Lambda | \bar{H} | \Phi^0 \rangle + \frac{1}{2} \langle \Lambda \left| \bar{\mathbf{V}} \cdot \mathbf{Q}_0 \left(\gamma^{CC} \right) \right| \Phi^0 \rangle \\ = &\ \langle \Lambda | \bar{H} | \Phi^0 \rangle + \frac{1}{2} \mathbf{V}_0 \left(\gamma^{CC} \right) \cdot \mathbf{Q}_0 \left(\gamma^{CC} \right) \end{aligned} \tag{7}$$

where $\bar{H}$ is the similarity transformed molecular Hamiltonian (see Equation 4) and γ^{CC} is the total CC density:

$$\gamma^{CC} = \gamma^0 + \gamma \tag{8}$$

where γ^0 is the reference density and γ is the CC reduced (or correlation) density. As we shall see below, the amplitudes for the deexcitation operator $\hat{\Lambda}$ play the role of Lagrange multipliers for the $\hat{T}$ amplitude equations. The last term on the right-hand side of Equation 7 is the solute-solvent interaction energy, and the factor of 1/2 accounts for the work to polarize the dielectric. Thus, the energy G_0 takes the form of a free energy because the averaging of the solvent degrees of freedom is accounted for implicitly in the dielectric permittivity, used to obtain the PCM charges $\mathbf{Q}(\gamma^{CC})$ through Equation 6.[4,59] The energy in Equation 7 can be separated in a reference and a correlation contribution, as for in vacuo CC:

$$G_0 = G^0 + \langle \Lambda \left| \bar{H}_N^{PCM} \right| \Phi^0 \rangle + \frac{1}{2} \mathbf{V}_N \cdot \mathbf{Q}_N \tag{9}$$

where G^0 is the reference energy, including the reference PCM charges:

$$G^0 = \langle \Phi^0 \left| \hat{H} \right| \Phi^0 \rangle + \frac{1}{2} \langle \Phi^0 \left| \hat{\mathbf{V}} \cdot \mathbf{Q}^0 \right| \Phi^0 \rangle \tag{10}$$

and $\bar{H}_N^{PCM}$ is

$$\bar{H}_N^{PCM} = \bar{H}_N + \bar{\mathbf{V}}_N \cdot \mathbf{Q}^0 \tag{11}$$

where we have written the PCM operator explicitly only for clarity; in practice, the solvent term in Equation 11 is included in the one-electron part of the normal-ordered Hamiltonian, that is, the molecular orbital (MO) energies when the canonical HF wave function is used as reference. Therefore, the solvent operator in Equation 11 does not generate any new term in the CC equations. In Equation 9, the correlation solute-solvent interaction energy only depends on the CC reduced one-particle density matrix (1PDM). From the computational cost standpoint, the solution of the reference equations in solution (called self-consistent reaction field equations, SCRF)[4] is about 20% more demanding than the in vacuo self-consistent field (SCF) equations. However, this extra effort is negligible compared to that for the solution of the CC equations, irrespective of the solvation scheme.

The PTED expression in Equation 7 has the disadvantage that the energy is quadratic in the CC density through the solvent term, which in turn means that the energy expression is quadratic in the $\hat{\Lambda}$ amplitudes. This implies that the evaluation of the CC-PCM-PTED energy requires the evaluation of both the $\hat{T}$ and $\hat{\Lambda}$ amplitudes, thus the two sets of equations to determine these amplitudes become coupled. This is different from the in vacuo case, where the energy is linear in $\hat{\Lambda}$, and these amplitudes are not necessary to obtain the energy. In our experience, the coupling of the $\hat{T}$ and $\hat{\Lambda}$ equations effectively makes the CC-PCM-PTED method 3–5 times more expensive the in vacuo CC, because both sets of equations must be solved iteratively until mutual polarization between solute and solvent is achieved.[42] The situation is even worse for excited states in the state-specific (SS) solvation formalism, because in the PTED scheme the ground and excited state amplitudes are all coupled.[27,46] This makes the calculations in solution significantly more computationally expensive than in vacuo.

Therefore, we suggested an approximation for the solute-solvent interaction energy that can eliminate this problem while preserving accuracy quantitatively.[44] This approximation is based on neglecting the interaction energy term that is quadratic in the $\hat{\Lambda}$ amplitudes. Expanding the interaction energy:

$$\begin{aligned}\mathbf{V}_N\cdot\mathbf{Q}_N = &\ \langle\Phi^0|\bar{\mathbf{V}}_N|\Phi^0\rangle\cdot\langle\Phi^0|\bar{\mathbf{Q}}_N|\Phi^0\rangle + 2\langle\Phi^0\left|\hat{\Lambda}\bar{\mathbf{V}}_N\right|\Phi^0\rangle\cdot\langle\Phi^0|\bar{\mathbf{Q}}_N|\Phi^0\rangle \\ &+ \langle\Phi^0\left|\hat{\Lambda}\bar{\mathbf{V}}_N\right|\Phi^0\rangle\cdot\langle\Phi^0\left|\hat{\Lambda}\bar{\mathbf{Q}}_N\right|\Phi^0\rangle \\ = &\ \mathbf{V}_N^T\cdot\mathbf{Q}_N^T + 2\mathbf{V}_N^\Lambda\cdot\mathbf{Q}_N^T + \mathbf{V}_N^\Lambda\cdot\mathbf{Q}_N^\Lambda\end{aligned} \tag{12}$$

where we have used the symmetry of the PCM $\mathbf{Y}$ matrix to collect the terms linear in $\hat{\Lambda}$, and we have defined a shorthand notation to distinguish the terms that depend on $\hat{\Lambda}$ from those that depend only on $\hat{T}$ (the former always depend on $\hat{T}$ through the similarity transformation of the operator, but we leave this implicit to simplify the notation). It is only the last term in Equation 12 that is responsible for the coupling of the $\hat{T}$ and $\hat{\Lambda}$ equations, thus we neglect it to obtain an energy expression that is linear in $\hat{\Lambda}$, as for in vacuo CC. The only PCM charges that survive are the $\mathbf{Q}_N^T$, which can be interpreted as the charges generated with the only part of the reduced 1PDM that does not depend on the $\hat{\Lambda}$ amplitudes, that is, the single excitation $\hat{T}$ amplitudes t_1. Therefore, we called this approximation PTES, where S stands for "singles". The CC-PCM-PTES energy expression is:

$$G_0^S = G^0 + \langle\Lambda\left|\bar{H}_N^{PCM}\right|\Phi^0\rangle + \frac{1}{2}\mathbf{V}_N^T\cdot\mathbf{Q}_N^T + \mathbf{V}_N^\Lambda\cdot\mathbf{Q}_N^T \tag{13}$$

The evaluation of G_0^S is achieved by minimizing the Lagrangian in Equation 13 with respect to the $\hat{\Lambda}$ amplitudes (λ_n) while keeping the reference wave function frozen, as for in vacuo CC:

$$\frac{\partial G_0^S}{\partial\lambda_n} = 0 = \langle\Phi^n\left|\bar{H}_N^{PCM} + \bar{\mathbf{V}}_N\cdot\mathbf{Q}_N^T\right|\Phi^0\rangle \tag{14}$$

These are the $\hat{T}$ equations, which allow one to evaluate the t_n amplitudes from Equation 1. Once the t_n amplitudes are computed, Equation 13 can be simplified to:

$$G_0^S = G^0 + \langle\Psi^0\left|\bar{H}_N^{PCM}\right|\Phi^0\rangle + \frac{1}{2}\mathbf{V}_N^T\cdot\mathbf{Q}_N^T \tag{15}$$

where the explicit dependence on $\hat{\Lambda}$ disappears, as for isolated molecules.[44] The $\hat{T}$ equations for CC-PCM-PTES are essentially identical to those of in vacuo noncanonical CC, because the explicit correlation solvent term is a

one-electron operator whose contributions look the same as those of a nondiagonal Fock operator.[60] Therefore, the explicit PCM terms add virtually no extra computational cost, because they can be folded into contractions that are already necessary in standard CC theory. In our implementation of CCSD-PCM, the cost of evaluating $\mathbf{Q}_N^T$ scales as $O(N^3)$, where N is the size of the basis set, because we need to transform the t_1 amplitudes in atomic orbital (AO) basis to use the standard PCM routines that solve Equation 6. Additionally, in our experience, the iterative procedure to solve Equation 14 converges in the same number of iterations as for in vacuo calculations. Thus, CC-PCM-PTES is virtually identical in cost to in vacuo CC. Hence, for the remaining of this work, we will focus the description of the CC-PCM theory only on the PTES scheme, and we will drop the S superscript in the following equations. We will discuss the quality of this approximation compared to the PTED scheme with a selection of examples in Section 3.

In order to evaluate molecular properties, analytical gradients of the CC-PCM-PTES energy in Equation 13 are necessary. As in standard CC theory, the gradients of the $\hat{T}$ amplitudes can be avoided by evaluating the $\hat{\Lambda}$ amplitudes first, so that the energy gradient can be expressed only in terms of the derivative of the MO coefficients, and of the one and two-electron integrals in AO basis, plus the derivative of the cavity terms.[55,60,61] The $\hat{\Lambda}$ amplitudes can be obtained by minimizing the energy in Equation 13 with respect to the t_n amplitudes. This leads to a system of linear equations similar to that for isolated molecules:

$$\frac{\partial G_0}{\partial t_n} = 0 = \langle \Lambda \left| \left[\bar{H}_N^{PCM} + \bar{\mathbf{V}}_N \cdot \mathbf{Q}_N^T, \hat{\tau}_n \right] \right| \Phi^0 \rangle + \langle \Phi^0 \left| \bar{\mathbf{V}}_N \cdot \mathbf{Q}_N^\Lambda \right| \Phi^n \rangle \tag{16}$$

where, as for the $\hat{T}$ equations, the PCM terms are identical in form to one-electron operators with noncanonical orbitals; therefore, they do not add any computational cost to the equations, and they are rather easy to implement. In Equation 16, the $\mathbf{Q}_N^T$ charges are fixed, as they are computed with the converged $\hat{T}$ amplitudes. However, the $\mathbf{Q}_N^\Lambda$ charges need to be updated together with the $\hat{\Lambda}$ amplitudes (although this is a system of linear equations, it is usually solved with iterative techniques due to the size of the matrices involved). The computational cost of evaluating the $\mathbf{Q}_N^\Lambda$ charges scales as $O(N^5)$, as that is the cost to evaluate the reduced 1PDM. Considering that the scaling of CCSD is $O(N^6)$, the added effort required to compute $\mathbf{Q}_N^\Lambda$ is negligible. Once the $\hat{T}$ and $\hat{\Lambda}$ amplitudes are evaluated, the same procedure used for in vacuo CC can be followed to obtain the derivative of the MO coefficients.[60,61] The derivation is rather lengthy, and we only report the terms due to the solvent that need to be added to the standard equations. The evaluation of the MO coefficient derivative requires the solution of the coupled perturbed HF (CPHF) equations,[62,63] a system of linear equations where the constant term is built with the proper combination of the reduced one and two-particle density matrices (1 and 2PDM).[60,61] Following the notation in References 26, 42, 44, the additional terms to the CPHF constant term are

$$\begin{aligned}
I_{km} &= -\left(\gamma_{kq} + \gamma_{qk}\right)\mathbf{V}_{qm} \cdot \mathbf{Q}_N + \left(\gamma_{kq}^\Lambda + \gamma_{qk}^\Lambda\right)\mathbf{V}_{qm} \cdot \mathbf{Q}_N^\Lambda \\
I_{ea} &= -\left(\gamma_{eq} + \gamma_{qe}\right)\mathbf{V}_{qa} \cdot \mathbf{Q}_N + \left(\gamma_{eq}^\Lambda + \gamma_{qe}^\Lambda\right)\mathbf{V}_{qa} \cdot \mathbf{Q}_N^\Lambda \\
I_{em} &= -\left(\gamma_{eq} + \gamma_{qe}\right)\mathbf{V}_{qm} \cdot \mathbf{Q}_N + \left(\gamma_{eq}^\Lambda + \gamma_{qe}^\Lambda\right)\mathbf{V}_{qm} \cdot \mathbf{Q}_N^\Lambda \\
I_{me} &= \left(\gamma_{mq} + \gamma_{qm}\right)\mathbf{V}_{qe} \cdot \mathbf{Q}_N^T - \left(\gamma_{mq}^\Lambda + \gamma_{qm}^\Lambda\right)\mathbf{V}_{qe} \cdot \mathbf{Q}_N^\Lambda
\end{aligned} \tag{17}$$

where $\mathbf{V}_{pq}$ is the matrix representation of the electrostatic potential operator in MO basis, γ_{pq} is the reduced 1PDM, see Equation 8, and $\gamma_{pq}^\Lambda = \gamma_{pq} - t_k^c \delta_{kp} \delta_{cq}$; the indexes k, m refer to occupied MOs, a, e to unoccupied MOs, and p, q to generic MOs. These expressions are slightly different than those presented in the original PTES paper,[44] where they were derived directly from the PCM-PTES energy in Equation 13. On the other hand, the expressions in Equation 17 reflect our implementation in the GAUSSIAN software,[64,65] and are based on the PCM-PTES energy written as the combination of terms quadratic in some density.

$$\frac{1}{2}\mathbf{V}_N^T \cdot \mathbf{Q}_N^T + \mathbf{V}_N^\Lambda \cdot \mathbf{Q}_N^T = \frac{1}{2}\mathbf{V}_N \cdot \mathbf{Q}_N - \frac{1}{2}\mathbf{V}_N^\Lambda \cdot \mathbf{Q}_N^\Lambda \tag{18}$$

Including the terms in Equation 17 in the CPHF equations allows one to obtain the PCM contribution to the MO derivatives. The computational cost of these PCM terms is negligible due to their $O(N^3)$ scaling. To complete the

derivative of the CC-PCM-PTES energy, the derivative of the electrostatic potential integrals and of the cavity terms must be added to the gradient[55]:

$$\left(\frac{1}{2}\mathbf{V}_N\cdot\mathbf{Q}_N-\frac{1}{2}\mathbf{V}_N^{\Lambda}\cdot\mathbf{Q}_N^{\Lambda}\right)^{[x]} = \gamma_{pq}\mathbf{V}_{pq}^{[x]}\cdot\mathbf{Q}_N+\frac{1}{2}\gamma_{pq}\mathbf{V}_{pq}\cdot\mathbf{Y}^{[x]}\cdot\gamma_{rs}\mathbf{V}_{rs} -\gamma'_{pq}\mathbf{V}_{pq}^{[x]}\cdot\mathbf{Q}_N-\frac{1}{2}\gamma'_{pq}\mathbf{V}_{pq}\cdot\mathbf{Y}^{[x]}\cdot\gamma'_{rs}\mathbf{V}_{rs} \tag{19}$$

where we have used again the symmetry of the PCM **Y** matrix. These derivative terms are essentially the same as those for time-dependent density functional theory (TDDFT) gradients in the presence of the solvent,[66] and the same routines can be utilized by using the CC 1PDM rather than the TDDFT 1PDM. Overall, the cost of adding the solvent to the CC equations is virtually negligible, as the extra terms are inexpensive to compute, and they do not significantly alter the in vacuo CC equations.

2.2 | Excited states

The theory of excited states for solvated molecules in hybrid methods follows two formalisms: the state specific (SS) and the linear response (LR).[67,68] The former is akin to the equation of motion CC (EOM-CC) formalism,[69] while the latter to the LR-CC formalism.[13,70] However, although in vacuo EOM-CC and LR-CC converge to the same equations for the excitation energies (albeit they still differ in the expressions for transition properties),[71,72] the inclusion of the solvent leads to two separate sets of equations, and to different values of the transition energy. The origin of the two formalisms has been discussed elsewhere,[67,68] and their main features can be summarized by saying that in the SS scheme the solvent responds to the excited state density of the solute, while in the LR scheme the solvent responds to the transition density between the ground and the excited state. Another complication with implicit solvation models such as PCM is the distinction between equilibrium and nonequilibrium regimes.[4] In a vertical excitation, the solvent molecules do not move fast enough to respond to the sudden change in the solute electron density, and the solvent polarization is only determined by the response of its electrons. This creates a nonequilibrium regime for the solute-solvent interaction. In continuum models, the difference in response time is modeled by separating the solvent polarization in two components: an inertial polarization that mimics the frozen position of the solvent molecules in equilibrium with the ground state solute density, and a dynamic polarization that mimics the response of the solvent electrons.[4] The latter is computed with the same PCM equation (see Equation 6), but with the static dielectric constant ε_0 replaced by the optical dielectric constant $\varepsilon_\infty = n^2$, where n is the refractive index of the medium. ε_∞ represents the high-frequency limit of the dielectric permittivity, $\varepsilon_\infty = \varepsilon(\omega \to \infty)$, and corresponds to an "instantaneous" response of the solvent electrons. This approximation is usually reasonable for describing the electrostatic polarization in vertical transitions, and ε_∞ is known for many solvents, so that PCM can be easily used to simulate a large number of experimental situations. When enough time is passed, of the order of the internal relaxation of the solute after a vertical excitation, the solute and solvent have enough time to mutually polarize, that is, the system relaxes to an equilibrium solvation regime, and the PCM equations can be solved again with ε_0. This is relevant when one is interested in finding the stationary points on the excited state potential energy surface (PES) of the solvated molecule. We developed the theory and implemented the computer code for the PTES approximation with the SS and LR formalisms in the equilibrium and nonequilibrium solvation regimes, including analytic gradients of the energy.[45,46,52,54] We will now discuss the main expressions for this series of approaches.

2.2.1 | State specific formalism

The CC-PCM-PTES method for excited states with the SS solvation formalism follows the EOM-CC theory for isolated molecules.[69] However, it is convenient to express the in vacuo energy for the K excited state in terms of a Lagrangian[46,73]:

$$E_K = E^0 + \langle\Lambda_K|\bar{H}_N|\Phi^0\rangle + \langle\Phi^0|\hat{L}_K\left[\bar{H}_N,\hat{R}_K\right]|\Phi^0\rangle + \omega_K\left(1-\langle\Phi^0|\hat{L}_K\hat{R}_K|\Phi^0\rangle\right) \tag{20}$$

where $\hat{L}_K$ and $\hat{R}_K$ are the Kth left and right-hand eigenvectors of $\bar{H}_N$ with eigenvalue ω_K, and $\hat{\Lambda}$ k is the equivalent of the ground state $\hat{\Lambda}$ operator. The last term on the right-hand side imposes the biorthonormality condition for the eigenstates of $\bar{H}_N$, which is non-Hermitian due to the similarity transformation.[69] In Equation 20, the $\hat{T}$ equations are obtained by minimizing E_K with respect to the $\hat{\Lambda}$ k amplitudes, and they are decoupled from any other amplitude equation. Once the $\hat{T}$ amplitudes are evaluated, one can diagonalize $\bar{H}_N$ from the right or from the left-hand sides, independently, to find the excitation energies ω_K and the related eigenvectors. In terms of the Lagrangian, the right-hand eigenvalue equation is obtained by minimization of E_K with respect to the $\hat{L}_K$ amplitudes, and vice versa. Finally, if one is interested in excited state properties or in the E_K gradients, the $\hat{\Lambda}$ k amplitudes must be evaluated by minimizing E_K with respect to the $\hat{T}$ amplitudes. A key point is that, in vacuo, all of these amplitude equations are decoupled from each other.

In the PTED-SS formalism, we can write a Lagrangian expression similar to that in Equation 20, but the full PCM energy couples the $\hat{T}$, $\hat{\Lambda}$ k, $\hat{R}_K$, and $\hat{L}_K$ amplitude equations because the solvent term is quadratic in the excited state density[46]:

$$\begin{aligned}\frac{1}{2}\mathbf{V}_{KN}\cdot\mathbf{Q}_{KN} = \; & \frac{1}{2}\mathbf{V}_N^K\cdot\mathbf{Q}_N^K + \mathbf{V}_N^K\cdot\mathbf{Q}_N^T + \frac{1}{2}\mathbf{V}_N^T\cdot\mathbf{Q}_N^T \\ & + \mathbf{V}_N^\Lambda\cdot\mathbf{Q}_N^T + \frac{1}{2}\mathbf{V}_N^\Lambda\cdot\mathbf{Q}_N^\Lambda + \mathbf{V}_N^\Lambda\cdot\mathbf{Q}_N^K\end{aligned} \tag{21}$$

where

$$\begin{aligned}\mathbf{Q}_{KN} = \; & \langle\Phi^0|\bar{\mathbf{Q}}_N|\Phi^0\rangle + \langle\Phi^0\left|\hat{\Lambda}_K\bar{\mathbf{Q}}_N\right|\Phi^0\rangle + \langle\Phi^0\left|\hat{L}_K\left[\bar{\mathbf{Q}}_N,\hat{R}_K\right]\right|\Phi^0\rangle \\ = \; & \mathbf{Q}_N^T + \mathbf{Q}_N^{\Lambda_K} + \mathbf{Q}_N^K\end{aligned} \tag{22}$$

and similarly for $\mathbf{V}_{KN}$. The coupling of all of the amplitude equations clearly increases the computational cost dramatically compared to the in vacuo case. Additionally, since the $\hat{T}$ equations must be solved in the presence of the excited state charges $\mathbf{Q}_{KN}$, $\hat{T}$ loses the meaning of ground state operator, and its amplitudes are just parameters of the excited state wave function.

In the PTES approximation, this coupling is eliminated by neglecting the last two terms on the right-hand side of Equation 21.[46] The energy Lagrangian in solution is:

$$\begin{aligned}G_K = \; & G^0 + \langle\Lambda_K\left|\bar{H}_N^{PCM}\right|\Phi^0\rangle + \langle\Phi^0\left|\hat{L}_K\left[\bar{H}_N^{PCM},\hat{R}_K\right]\right|\Phi^0\rangle \\ & + \omega_K\left(1-\langle\Phi^0\left|\hat{L}_K\hat{R}_K\right|\Phi^0\rangle\right) + \frac{1}{2}\mathbf{V}_N^{TK}\cdot\mathbf{Q}_N^{TK} + \mathbf{V}_N^{\Lambda_K}\cdot\mathbf{Q}_N^T\end{aligned} \tag{23}$$

where $\mathbf{Q}_N^{TK} = \mathbf{Q}_N^T + \mathbf{Q}_N^K$. Minimizing G_K with respect to the $\hat{\Lambda}$ k amplitudes, we obtain the $\hat{T}$ amplitudes equations in Equation 14. Minimization with respect to the $\hat{L}_K$ amplitudes leads to the $\hat{R}_K$ equations, and vice versa:

$$\frac{\partial G_K}{\partial l_{K,n}} = \langle\Phi^n\left|\left[\bar{H}_N^{PCM} + \bar{\mathbf{V}}_N\cdot\mathbf{Q}_N^{TK},\hat{R}_K\right]\right|\Phi^0\rangle - \omega_K\langle\Phi^n\left|\hat{R}_K\right|\Phi^0\rangle = 0 \tag{24}$$

$$\frac{\partial G_K}{\partial r_{K,n}} = \langle\Phi^0\left|\hat{L}_K\left[\bar{H}_N^{PCM} + \bar{\mathbf{V}}_N\cdot\mathbf{Q}_N^{TK},\hat{\tau}_n\right]\right|\Phi^0\rangle - \omega_K\langle\Phi^0\left|\hat{L}_K\right|\Phi^n\rangle = 0 \tag{25}$$

These expressions are in the form of a non-Hermitian eigenvalue problem, and can be solved with iterative algorithms to extract the lowest few eigenvectors. Although the $\hat{T}$ equations are decoupled from the rest, the solvent energy couples the $\hat{L}_K$ and $\hat{R}_K$ equations through the $\mathbf{Q}_N^K$ charges. The computational cost of the PCM terms is still negligible compared to the standard EOM-CC terms, as the most expensive part scales as $O(N^5)$, i.e., the evaluation of the partial excited state reduced 1PDM:

$$\gamma_{pq}^{K} = \langle \Phi^0 \left| \hat{L}_K \left[\{ p^\dagger q \}, \hat{R}_K \right] \right| \Phi^0 \rangle \tag{26}$$

where we have used a second quantization notation for the creation and annihilation operators, and curly brackets represent normal ordering. The density in Equation 26 is used to compute the $\mathbf{Q}_N^K$ charges through the PCM equation (see Equation 6). The evaluation of these three sets of amplitudes ($\hat{T}$, $\hat{L}_K$, and $\hat{R}_K$) is sufficient to obtain the excited state energy, and Equation 23 simplifies to:

$$G_K = G_0 + \omega_K - \frac{1}{2}\mathbf{V}_N^K \cdot \mathbf{Q}_N^K \tag{27}$$

As mentioned above, vertical excitations require the nonequilibrium regime, for which the energy expression can be formally written in terms of the ground state dynamic and inertial charges, and the excited state dynamic charge contributions[45]:

$$\begin{aligned} G_K^{neq} = \; & G^0 + \langle \Lambda_K \left| \bar{H}_N^{PCM} \right| \Phi^0 \rangle + \langle \Phi^0 \left| \hat{L}_K \left[\bar{H}_N^{PCM}, \hat{R}_K \right] \right| \Phi^0 \rangle + \omega_K \left(1 - \langle \Phi^0 \left| \hat{L}_K \hat{R}_K \right| \Phi^0 \rangle \right) \\ & + \frac{1}{2}\mathbf{V}_N^{TK} \cdot \mathbf{Q}_N^{TK,dyn} + \mathbf{V}_N^{\Lambda} \cdot \mathbf{Q}_N^{T,dyn} + \mathbf{V}_{KN} \cdot \mathbf{Q}_N^{T,in} - \frac{1}{2}\mathbf{V}_N^{T} \cdot \mathbf{Q}_N^{T,in} \end{aligned} \tag{28}$$

where $\mathbf{Q}_N^{TK,dyn} = \mathbf{Q}_N^T + \mathbf{Q}_N^{K,dyn}$, and the charges $\mathbf{Q}_N^{K,dyn}$ are computed using the same density in Equation 26, but with the optical dielectric constant ε_∞ in the PCM equations, see Equation 6. Minimization of G_K^{neq} with respect to the $\hat{\Lambda}$ k amplitudes leads again to Equation 14 for the $\hat{T}$ amplitudes. The left and right-hand eigenvectors are computed through expressions similar to those in Equations 24–25 with the substitution $\mathbf{Q}_N^{TK} \rightarrow \mathbf{Q}_N^{TK,dyn}$. Therefore, the same code that computes the equilibrium excited state energy can be used to evaluate the nonequilibrium energy. Finally, at convergence, the nonequilibrium energy is simply:

$$G_K^{neq} = G^0 + \omega_K - \frac{1}{2}\mathbf{V}_N^K \cdot \mathbf{Q}_N^{K,dyn} \tag{29}$$

Thus, both in the equilibrium and nonequilibrium regimes, the evaluation of the energy does not require the $\hat{\Lambda}$ k amplitudes. However, the latter are necessary to perform geometry optimization on the excited state PES, which require the gradient of G_K in Equation 23. The $\hat{\Lambda}$ k equations are obtained by minimizing G_K with respect to the $\hat{T}$ amplitudes:

$$\begin{aligned} \frac{\partial G_K}{\partial t_n} = 0 = \; & \langle \Lambda \left| \left[\bar{H}_N^{PCM} + \bar{\mathbf{V}}_N \cdot \mathbf{Q}_N^T, \hat{\tau}_n \right] \right| \Phi^0 \rangle + \langle \Phi^0 \left| \bar{\mathbf{V}}_N \cdot \mathbf{Q}_N^{\Lambda K} \right| \Phi^n \rangle \\ & \langle \Phi^0 \left| \hat{L}_K \left[\left[\bar{H}_N^{PCM} + \bar{\mathbf{V}}_N \cdot \mathbf{Q}_N^{TK}, \hat{R}_K \right], \hat{\tau}_n \right] \right| \Phi^0 \rangle \end{aligned} \tag{30}$$

where $\mathbf{Q}_N^{\Lambda K} = \mathbf{Q}_N^{\Lambda} + \mathbf{Q}_N^K$. This expression is similar to that for the ground state $\hat{\Lambda}$ amplitudes, see Equation 16, except for the extra constant term with the nested double commutator. Equation 30 is also similar to the excited state $\hat{\Lambda}$ k equation for in vacuo CC, with a few extra PCM terms.[73] The $\mathbf{Q}_N^{TK}$ contribution in the double commutator constant term can be easily folded in contractions already necessary in the in vacuo CC equations, therefore it does not increase the computational cost. As for the ground state, the only charges that need to be updated during the iterative procedure to solve Equation 30 are the $\mathbf{Q}_N^{\Lambda}$ charges, and the same computational considerations apply here as well. Once again, PCM also adds a series of contributions to the constant term of the CPHF equations to evaluate the derivative of the MO coefficients, and some direct contributions to the gradient for the derivative of the electrostatic potential integrals and the PCM matrix.[46] All of these contributions are easy to derive and implement, if the PCM-PTES-SS energy is written as:

$$\frac{1}{2}\mathbf{V}_N^{TK} \cdot \mathbf{Q}_N^{TK} + \mathbf{V}_N^{\Lambda} \cdot \mathbf{Q}_N^{T} = \frac{1}{2}\mathbf{V}_{KN} \cdot \mathbf{Q}_{KN} + \frac{1}{2}\mathbf{V}_N^K \cdot \mathbf{Q}_N^K - \frac{1}{2}\mathbf{V}_N^{\Lambda K} \cdot \mathbf{Q}_N^{\Lambda K} \tag{31}$$

i.e., as a combination of terms quadratic in some density. In this way, the extension of Equations 17 and 19 to the excited state case is straightforward.[46]

Once the minimum energy geometry in the excited state PES is determined, a vertical emission energy can be computed to compare with fluorescence spectra. As in absorption, a nonequilibrium regime is established also in emission. This requires the evaluation and storage of the inertial excited state charges:

$$\mathbf{Q}^{K,in} = \left(\mathbf{Q}^0 + \mathbf{Q}_N^{TK}\right)^{in} \tag{32}$$

which are obtained from the difference between the total and dynamic charges: $\mathbf{Q}^{in} = \mathbf{Q} - \mathbf{Q}^{dyn}$, and the latter are computed with Equation 6 by using ε_∞. Then, a ground state nonequilibrium calculation is performed in the presence of the nonequilibrium charges. This requires two steps. First, a nonequilibrium reference calculation provides the reference energy:

$$G^{0,neq} = \langle \Phi^0 | \hat{H} | \Phi^0 \rangle + \frac{1}{2}\mathbf{V}^0 \cdot \mathbf{Q}^{0,dyn} + \mathbf{V}^0 \cdot \mathbf{Q}^{K,in} - \frac{1}{2}\mathbf{V}^K \cdot \mathbf{Q}^{0,in} \tag{33}$$

where $\mathbf{V}^K = \mathbf{V}^0 + \mathbf{V}_N^{TK}$. Second, the CC nonequilibrium energy is obtained by minimizing the following Lagrangian with respect to the $\hat{\Lambda}$ amplitudes:

$$G_0^{neq} = G^{0,neq} + \langle \Lambda \left| \bar{H}_N^{PCM,neq} \right| \Phi^0 \rangle + \frac{1}{2}\mathbf{V}_N^T \cdot \mathbf{Q}_N^{T,dyn} + \mathbf{V}_N^\Lambda \cdot \mathbf{Q}_N^{T,dyn} \tag{34}$$

where

$$\bar{H}_N^{PCM,neq} = \bar{H}_N + \bar{\mathbf{V}}_N \cdot \left(\mathbf{Q}^{0,dyn} + \mathbf{Q}^{K,in}\right) \tag{35}$$

The expression in Equation 34 is essentially identical to that for the equilibrium case, see Equation 13, except for the values of the orbital energies and MO coefficients, and for the fact that the correlation charges $\mathbf{Q}_N^T$ are computed with ε_∞ rather than ε_0. Therefore, the same computer code can be straightforwardly reused, and the same considerations about computational cost apply.[45]

In summary, excited state solvation with the SS formalism is similar to the in vacuo case, but with a few important differences. One needs to decide first whether the calculation needs to be performed in the equilibrium or nonequilibrium regimes. The equations in the two cases are very similar, but the solvent response can be very different for polar solvents due to the difference in magnitude between ε_0 and ε_∞. The explicit PCM terms, both in the energy, amplitude, and gradient expressions are similar to those of a one-electron operator in a noncanonical MO basis. Thus, they do not directly lead to an increase in computational cost. However, in the SS formalism, the solvent energy couples the $\hat{L}_K$ and $\hat{R}_K$ amplitude equations, Equations 24–25, because of the $\mathbf{Q}_N^K$ charges. These two sets of equations must be solved simultaneously until mutual polarization between the solute and the solvent is achieved, which can take several PCM macro-iterations if the solute excited state density is very different from the ground state density. Different SS equations must be solved for different excited states, contrary to the case of an isolated molecule, where multiple excitation energies can be computed simultaneously through the partial diagonalization of $\bar{H}_N$. Nonetheless, this extra cost is still small compared to the full PTED-SS scheme, where all sets of CC amplitudes are coupled ($\hat{T}$, $\hat{\Lambda}$ k, $\hat{R}_K$, and $\hat{L}_K$). Furthermore, the PTES scheme allows one to evaluate transition properties within the EOM-CC approach,[69] because the ground state is orthogonal to the *K*th excited state, while this is not the case in the PTED scheme (however, in neither approach excited states are orthogonal to each other, because they are evaluated with state-specific charges). In this respect, the PTES approximation is better defined than the PTED scheme thanks to the decoupling of the ground state $\hat{T}$ amplitudes from the excited state equations, as for in vacuo EOM-CC. The PTES-SS scheme can be considered the CC equivalent of the vertical excitation model (VEM) developed in the contest of TDDFT-PCM.[74]

2.2.2 | Linear response formalism

In the LR formalism, the excitation energies are obtained as the poles of the LR function of the electronic ground state in the presence of an external field.[13] These poles are obtained by diagonalizing the Jacobian matrix, that is, the mixed-energy second derivative matrix[52]:

$$\frac{\partial^2 G_0}{\partial t_n \partial \lambda_m} = \langle \Phi^m \left| \left[\bar{H}_N^{PCM} + \bar{\mathbf{V}}_N \cdot \mathbf{Q}_N^T, \hat{\tau}_n \right] \right| \Phi^0 \rangle + \langle \Phi^m | \bar{\mathbf{V}}_N | \Phi^0 \rangle \cdot \langle \Phi^0 | [\bar{\mathbf{Q}}_N, \hat{\tau}_n] | \Phi^0 \rangle \tag{36}$$

Since the Jacobian matrix in Equation 36 is not Hermitian, it has different left ($\hat{L}_K$) and right-hand ($\hat{R}_K$) eigenvectors, related by biorthogonality. The eigenvalue equations for the two sets of eigenvectors are:

$$\langle \Phi^n \left| \left[\bar{H}_{0N}^{PCM} + \bar{\mathbf{V}}_N \cdot \mathbf{Q}_N^T, \hat{R}_K \right] \right| \Phi^0 \rangle + \langle \Phi^n \left| \bar{\mathbf{V}}_N \cdot \mathbf{Q}_N^{R_K} \right| \Phi^0 \rangle = \omega_K \langle \Phi^n \left| \hat{R}_K \right| \Phi^0 \rangle \tag{37}$$

$$\langle \Phi^0 \left| \hat{L}_K \left[\bar{H}_{0N}^{PCM} + \bar{\mathbf{V}}_N \cdot \mathbf{Q}_N^T, \hat{\tau}_n \right] \right| \Phi^0 \rangle + \langle \Phi^0 \left| \left[\bar{\mathbf{V}}_N \cdot \mathbf{Q}_N^{L_K}, \hat{\tau}_n \right] \right| \Phi^0 \rangle = \omega_K \langle \Phi^0 \left| \hat{L}_K \right| \Phi^n \rangle \tag{38}$$

where in both cases, ω_K is the excitation energy, and the transition charges are:

$$\begin{aligned} \mathbf{Q}_N^{R_K} &= \langle \Phi^0 \left| \left[\bar{\mathbf{Q}}_N, \hat{R}_K \right] \right| \Phi^0 \rangle \\ \mathbf{Q}_N^{L_K} &= \langle \Phi^0 \left| \hat{L}_K \bar{\mathbf{Q}}_N \right| \Phi^0 \rangle \end{aligned} \tag{39}$$

Note that the right-hand charges $\mathbf{Q}_N^{R_K}$ are different between the PTES and PTED schemes, because in the latter the bra is $\langle \Lambda |$.[49,52] More importantly, in the PTED method, the quadratic form of the solvent energy (see Equation 9), couples the equations for the response of the $\hat{T}$ and $\hat{\Lambda}$ amplitudes. This is usually avoided by neglecting this coupling in the response equations, which leads to a somewhat inconsistent treatment of the energy and linear response function.[12,28] On the other hand, the $\hat{T}$ and $\hat{\Lambda}$ equations are decoupled from the very beginning in the PTES scheme, see Equation 13, and there is no inconsistency with the LR function. In terms of computational cost, the evaluation of the $\mathbf{Q}_N^{R_K}$ and $\mathbf{Q}_N^{L_K}$ charges in Equation 39 scales as $O(N^5)$, due to the scaling of the evaluation of the transition density. The cost of the explicit PCM terms in Equations 37–38 is again negligible, as these are one-electron operators than can be folded into intermediates already necessary for the standard LR-CC calculation. An advantage of the LR formalism over the SS one is that, since the response charges depend on the transition rather than the state density, multiple states can be treated simultaneously as for isolated molecules. Therefore, the computational cost of the CC-PCM-PTES-LR scheme is virtually the same as that of in vacuo LR-CC.

Contrary to the SS case, where transition properties are computed with a frozen-$\hat{T}$ approximation,[69] in LR these properties are evaluated from the residues of the linear response function, which do take into account the response of the $\hat{T}$ amplitudes.[71,72] This response is obtained by defining a new deexcitation operator $\hat{M}_K$, whose amplitudes are obtained by solving a linear system of equations similar to that for the $\hat{\Lambda}$ amplitudes[52]:

$$\begin{aligned} &\langle \Lambda \left| \left[\left[\bar{H}_N^{PCM} + \bar{\mathbf{V}}_N \cdot \mathbf{Q}_N^T, \hat{R}_K \right], \hat{\tau}_n \right] \right| \Phi^0 \rangle \\ &+ \langle \Phi^0 \left| \left[\bar{\mathbf{V}}_N \cdot \mathbf{Q}_N^{\Lambda - R_K}, \hat{\tau}_n \right] \right| \Phi^0 \rangle + \langle \Lambda \left| \left[\bar{\mathbf{V}}_N \cdot \mathbf{Q}_N^{R_K}, \hat{\tau}_n \right] \right| \Phi^0 \rangle \\ &+ \langle \Phi^0 \left| \hat{M}_K \left[\bar{H}_N^{PCM} + \bar{\mathbf{V}}_N \cdot \mathbf{Q}_N^T, \hat{\tau}_n \right] \right| \Phi^0 \rangle \\ &+ \langle \Phi^0 \left| \left[\bar{\mathbf{V}}_N \cdot \mathbf{Q}_N^{M_K}, \hat{\tau}_n \right] \right| \Phi^0 \rangle + \omega_K \langle \Phi^0 \left| \hat{M}_K \right| \Phi^n \rangle = 0 \end{aligned} \tag{40}$$

where

$$\begin{aligned} \mathbf{Q}_N^{\Lambda - R_K} &= \langle \Phi^0 \left| \Lambda \left[\bar{\mathbf{Q}}_N, \hat{R}_K \right] \right| \Phi^0 \rangle \\ \mathbf{Q}_N^{M_K} &= \langle \Phi^0 \left| \hat{M}_K \bar{\mathbf{Q}}_N \right| \Phi^0 \rangle \end{aligned} \tag{41}$$

The transition moments are evaluated as:

$$\begin{aligned} T_{0K}^X &= \langle \Lambda \left| \left[\bar{X}, \hat{R}_K \right] \right| \Phi^0 \rangle + \langle \Phi^0 \left| \hat{M}_K \bar{X} \right| \Phi^0 \rangle \\ T_{K0}^X &= \langle \Phi^0 \left| \hat{L}_K \bar{X} \right| \Phi^0 \rangle \end{aligned} \tag{42}$$

which are then combined to compute the transition property of interest

$$S_{0K}^{XY} = \frac{1}{2}\left(T_{0K}^{X} T_{K0}^{Y} + T_{0K}^{Y} T_{K0}^{X}\right) \tag{43}$$

where X and Y are particular perturbations; for instance, if $X = Y = \mu$, where μ is the electric dipole, then S_{0K}^{XY} is the dipole strength between the ground state and the Kth excited state.[12,28] The expression in Equation 40 has many elements in common with that for $\hat{\Lambda}$ k in Equation 30, as for in vacuo LR-CC, although the PCM charges are computed with different density matrices. In Equation 40, the only charges that change during the iterative solution are $\mathbf{Q}_N^{M_K}$, while the others are fixed. As for the other sets of equations, the scaling of the PCM contributions is of the order of $O(N^5)$ for the evaluation of the density corresponding to the $\mathbf{Q}_N^{M_K}$ charges. Transition properties computed as residues of the linear response function require the solution of one set of $\hat{M}_K$ linear equations (Equation 40) for each excited state, as in in vacuo LR-CC.[13,70,71,73] Since the scaling of these equations is $O(N^6)$, the added computational effort is considerable, and a more efficient alternative is to revert to the approximate EOM-CC approach.[69,72] Nonequilibrium vertical excitation calculations are easily performed in the LR formalism, by evaluating the excited state charges in Equations 39 and 41 with the optical dielectric constant ε_∞ instead of the static constant ε_0.

The excited state energy with the LR formalism is:

$$G_K = G_0 + \omega_K \tag{44}$$

which is different than the SS energy in Equation 27, or in Equation 29 for the nonequilibrium case, because the LR formalism does not include the full mutual polarization between the excited solute and the solvent. However, the low computational cost of the LR formalism makes it attractive for the exploration of the excited state PES, which requires the evaluation of the derivative of the energy with respect to nuclear displacements. It is useful to recast the expression in Equation 44 in terms of an energy Lagrangian[54,73]:

$$\begin{aligned} G_K = \;& G^0 + \langle \Lambda_K \left| \bar{H}_{0N}^{PCM} \right| \Phi^0 \rangle + \frac{1}{2}\mathbf{V}_N^T \cdot \mathbf{Q}_N^T + \mathbf{V}_N^{\Lambda_K} \cdot \mathbf{Q}_N^T \\ & + \langle \Phi^0 \left| \hat{L}_K \left[\bar{H}_{0N}^{PCM} + \bar{\mathbf{V}}_N \cdot \mathbf{Q}_N^T, \hat{R}_K \right] \right| \Phi^0 \rangle \\ & + \mathbf{V}_N^{L_K} \cdot \mathbf{Q}_N^{R_K} + \omega_K \left(1 - \langle \Phi^0 \left| \hat{L}_K \hat{R}_K \right| \Phi^0 \rangle\right) \end{aligned} \tag{45}$$

The $\hat{\Lambda}$ k amplitudes play again the role of Lagrangian multipliers for the $\hat{T}$ amplitude equations, such that the minimization of G_K in Equation 45 returns Equation 14. Minimization of G_K with respect to the $\hat{L}_K$ and $\hat{R}_K$ amplitudes leads to the eigenvalue equations for the eigenvectors in Equations 37–38. Minimization of G_K with respect to the $\hat{T}$ amplitudes leads to the $\hat{\Lambda}$ k equations[54]:

$$\begin{aligned} \frac{\partial G_K}{\partial t_n} = 0 = \;& \langle \Phi^0 \left| \bar{H}_N^{PCM} + \bar{\mathbf{V}}_N \cdot \mathbf{Q}_N^{T\Lambda_K K} \right| \Phi^n \rangle + \langle \Phi^0 \left| \left[\hat{\Lambda}_K, \bar{H}_{0N}^{PCM} + \bar{\mathbf{V}}_N \cdot \mathbf{Q}_N^T \right] \right| \Phi^n \rangle \\ & + \langle \Phi^0 \left| \bar{H}_N^{PCM} + \bar{\mathbf{V}}_N \cdot \mathbf{Q}_N^T \right| \tilde{\Phi} \rangle \langle \tilde{\Phi} \left| \hat{\Lambda}_K \right| \Phi^n \rangle \\ & + \langle \Phi^0 \left| \hat{L}_K \left[\left[\bar{H}_N^{PCM} + \bar{\mathbf{V}}_N \cdot \mathbf{Q}_N^T, \hat{R}_K \right], \hat{\tau}_n \right] \right| \Phi^0 \rangle \\ & + \langle \Phi^0 \left| \hat{L}_K \left[\bar{\mathbf{V}}_N \cdot \mathbf{Q}_N^{R_K}, \hat{\tau}_n \right] \right| \Phi^0 \rangle + \langle \Phi^0 \left| \left[\left[\bar{\mathbf{V}}_N \cdot \mathbf{Q}_N^{L_K}, \hat{R}_K \right], \hat{\tau}_n \right] \right| \Phi^0 \rangle \end{aligned} \tag{46}$$

where $\mathbf{Q}_N^{T\Lambda_K K} = \mathbf{Q}_N^T + \mathbf{Q}_N^{\Lambda_K} + \mathbf{Q}_N^K$ and $\left|\tilde{\Phi}\right\rangle\left\langle\tilde{\Phi}\right|$ represent a sum over all excited determinants within the chosen truncation of the cluster amplitudes (e.g., for CCSD the sum is over all singly and doubly excited determinants). As for in vacuo LR-CC,[73] the evaluation of the perturbation-independent $\hat{\Lambda}$ k amplitudes avoids the need to evaluate the derivative of the $\hat{T}$ amplitudes for each perturbation, such that the G_K gradient can be written in terms of the derivative of the integrals in AO basis, of the MO coefficients, and of the PCM cavity. However, while for isolated molecules the $\hat{\Lambda}$ k equations are the same for the EOM-CC and LR-CC formalisms,[73] these equations are different for SS and LR solvation, compare Equations 30 and 46. Specifically, the LR $\hat{\Lambda}$ k equations have more terms due to the asymmetric PCM energy contribution ($\mathbf{V}_N^{L_K} \cdot \mathbf{Q}_N^{R_K}$ in Equation 45), which leads to the last two terms on the right-hand side of Equation 46. Once

the $\hat{\Lambda}$ k equations are solved, the evaluation of the energy gradients proceeds as for isolated molecules: the 1 and 2PDM are constructed and assembled for the constant term of the CPHF Equations.[60,61] The first three PCM terms in Equation 45 can be recast in a form quadratic in some density[54]:

$$\begin{aligned}&\frac{1}{2}\mathbf{V}_N^T\cdot\mathbf{Q}_N^T+\mathbf{V}_N^{\Lambda_K}\cdot\mathbf{Q}_N^T+\mathbf{V}_N^K\cdot\mathbf{Q}_N^T\\&=\frac{1}{2}\mathbf{V}_N^{T\Lambda_K K}\cdot\mathbf{Q}_N^{T\Lambda_K K}-\frac{1}{2}\mathbf{V}_N^{\Lambda_K K}\cdot\mathbf{Q}_N^{\Lambda_K K}\end{aligned}\tag{47}$$

so that contributions similar to those in Equation 17 need to be computed for the CPHF, and in Equation 19 for the electrostatic potential and cavity derivatives. The nonsymmetric term, $\mathbf{V}_N^{L_K}\cdot\mathbf{Q}_N^{R_K}$, leads to new terms for the CPHF equations[54]:

$$\begin{aligned}I_{ij}^{L/R}=&-\left(\gamma_{tj}^{L_K}+\gamma_{jt}^{L_K}\right)\mathbf{V}_{it}\cdot\mathbf{Q}_N^{R_K}-\left(\gamma_{tj}^{R_K}+\gamma_{jt}^{R_K}\right)\mathbf{V}_{it}\cdot\mathbf{Q}_N^{L_K}\\I_{ab}^{L/R}=&-\left(\gamma_{tb}^{L_K}+\gamma_{bt}^{L_K}\right)\mathbf{V}_{ta}\cdot\mathbf{Q}_N^{R_K}-\left(\gamma_{tb}^{R_K}+\gamma_{bt}^{R_K}\right)\mathbf{V}_{ta}\cdot\mathbf{Q}_N^{L_K}\\I_{ai}^{L/R}=&-\left(\gamma_{ta}^{L_K}+\gamma_{at}^{L_K}\right)\mathbf{V}_{it}\cdot\mathbf{Q}_N^{R_K}-\left(\gamma_{ta}^{R_K}+\gamma_{at}^{R_K}\right)\mathbf{V}_{it}\cdot\mathbf{Q}_N^{L_K}\\I_{ia}^{L/R}=&\left(\gamma_{ti}^{L_K}+\gamma_{it}^{L_K}\right)\mathbf{V}_{ta}\cdot\mathbf{Q}_N^{R_K}+\left(\gamma_{ti}^{R_K}+\gamma_{it}^{R_K}\right)\mathbf{V}_{ta}\cdot\mathbf{Q}_N^{L_K}\end{aligned}\tag{48}$$

and for the direct contributions to the gradient:

$$\left(\mathbf{V}_N^{L_K}\cdot\mathbf{Q}_N^{R_K}\right)^{[x]}=\gamma_{rs}^{L_K}\mathbf{V}_{rs}^{[x]}\cdot\mathbf{Q}_N^{R_K}+\gamma_{rs}^{R_K}\mathbf{V}_{rs}^{[x]}\cdot\mathbf{Q}_N^{L_K}+\gamma_{rs}^{L_K}\mathbf{V}_{rs}\cdot\mathbf{Y}^{[x]}\cdot\mathbf{V}_{rs}\gamma_{rs}^{R_K}\tag{49}$$

Overall, these additional PCM terms are computationally inexpensive, and they add no detectable cost to the calculation. Once a minimum energy structure is found on the solute excited state PES, a vertical emission calculation in the nonequilibrium solvation regime can be evaluated in a similar way as for the SS formalism, see Equations 32–34.

The LR formalism can be also used to evaluate certain molecular properties, such as the electric polarizability or the specific rotation in chiral compounds.[52,75,76] The LR function for the PTES approximation takes the form[52]:

$$\begin{aligned}\langle\langle X;Y\rangle\rangle_\omega=&\frac{1}{2}\hat{C}^{\pm\omega}\hat{P}(XY)[\langle\Lambda\left|\left[\bar{X},\hat{T}_\omega^Y\right]\right|\Phi^0\rangle+\frac{1}{2}\langle\Lambda\left|\left[\left[\bar{H}_{0N}^{PCM}+\bar{\mathbf{V}}_N\cdot\mathbf{Q}_N^T,\hat{T}_{-\omega}^X\right],\hat{T}_\omega^Y\right]\right|\Phi^0\rangle\\&+\frac{1}{2}\mathbf{V}_{N,-\omega}^{T^X}\cdot\mathbf{Q}_{N,\omega}^{T^Y}+\mathbf{V}_{N,-\omega}^{\Lambda-T^X}\cdot\mathbf{Q}_{N,\omega}^{T^Y}]\end{aligned}\tag{50}$$

where ω is the frequency of the impinging light, the operator $\hat{C}^{\pm\omega}$ takes the sum of the entire expression and of its complex conjugate, and the operator $\hat{P}(XY)$ symmetrizes the expression with respect to the interchange of X and Y. The perturbed $\hat{T}$ amplitudes are obtained by solving the following linear system of equations:

$$\begin{aligned}&\langle\Phi^n\left|\left[\bar{H}_{0N}^{PCM}+\bar{\mathbf{V}}_N\cdot\mathbf{Q}_N^T,\hat{T}_\omega^Y\right]\right|\Phi^0\rangle-\omega\langle\Phi^n\left|\hat{T}_\omega^Y\right|\Phi^0\rangle\\&+\langle\Phi^n\left|\bar{\mathbf{V}}_N\cdot\mathbf{Q}_{N,\omega}^{T^Y}\right|\Phi^0\rangle=-\langle\Phi^n|\bar{Y}|\Phi^0\rangle\end{aligned}\tag{51}$$

The charges and electrostatic potential that depend on the perturbed $\hat{T}$ amplitudes in Equations 50–51 (e.g., $\mathbf{Q}_{N,\omega}^{T^Y}$) are computed as the charges $\mathbf{Q}_N^{R_K}$ in Equation 39, but with the perturbed $\hat{T}$ amplitudes (e.g., $\hat{T}_\omega^Y$).[52] Similarly, $\mathbf{V}_{N,-\omega}^{\Lambda-T^X}$ in Equation 50 is computed as in Equation 41. If $X=Y=\mu$, the LR function in Equation 50 provides the various elements of the electric dipole polarizability tensor, while if $X=\mu$ and $Y=m$ (where m is the magnetic dipole), one obtains the elements of the Rosenfeld tensor, whose trace is proportional to the specific rotation.[52,75,76] As for the excitation energies, the perturbed $\hat{T}$ and $\hat{\Lambda}$ amplitudes are automatically decoupled in the PTES approximation, and the extra PCM terms in Equations 50–51 add negligible computational cost compared to the in vacuo LR-CC method.

In summary, the PTES-LR formalism allows one to include explicit solvation effects both in the reference and in the CC wave function equations without a significant increase in the computational effort. Based on our current experience, the solvent model does not affect the rate of convergence of the iterative solution of the amplitude equations. Therefore, ground and excited state as well as response calculations with the LR-CC-PCM-PTES method are virtually identical in cost to the corresponding in vacuo LR-CC calculations.

2.3 | Polarizable force fields

The theoretical framework developed in the previous sections can also be applied to classical polarizable force fields (MMPol) where the energy can be expressed in a form quadratic in the QM density. We combined CC methods with MMPol based on the fluctuating charges (FQ) model[48] and the induced dipole (ID) model.[53] In the former, each polarizable site is endowed with a point charge whose magnitude can vary depending on the mutual polarization with the QM region and the rest of the environment. This approach is quite similar to PCM, except that the charges are distributed on actual molecular units rather than on the cavity surface that separates the solute from the continuum dielectric representing the solvent. In the FQ model, the charges depend on two empirical parameters, the atomic hardness and electronegativity, rather than the dielectric constant of the solvent as in PCM.[77] The ID model is based on fixed point charges and induced atomic dipoles on each polarizable site, so that the interaction is with the electric field generated by the QM region (and the other dipoles) on each individual site.[78–80] We are going to use the latter approach to describe the main concepts and the similarities with the CC-PCM theory.[53]

The energy of the environment can be written as:

$$E^{Env}\left(\gamma,\vec{\boldsymbol{\mu}}\right)=E^{MM}+E^{QM/MM}(\gamma)+E^{Pol}\left(\gamma,\vec{\boldsymbol{\mu}}\right) \tag{52}$$

where γ is the QM density, and $\vec{\boldsymbol{\mu}}$ collects the induced dipoles on all polarizable sites. The first two terms on the right-hand site of Equation 52 are the MM energy and the interaction energy with the QM region for the nonpolarizable part of the force field, respectively. These two terms do not enter the CC equations because E^{MM} is a classical term like the nuclear-nuclear repulsion, and $E^{QM/MM}(\gamma)$ is a fixed one electron term that is included in the Fock matrix like the electron-nuclear attraction term. The only contribution to E^{Env} that is relevant for the CC equations is the last one in Equation 52, the polarization energy:

$$E^{Pol}\left(\gamma,\vec{\boldsymbol{\mu}}\right)=-\vec{\boldsymbol{\mu}}\cdot\left[\vec{\mathbf{E}}^{MM}+\vec{\mathbf{E}}^{QM}(\gamma)\right]+\frac{1}{2}\vec{\boldsymbol{\mu}}\cdot\mathbf{T}(\boldsymbol{\alpha})\vec{\boldsymbol{\mu}} \tag{53}$$

where $\vec{\mathbf{E}}$ is the electric field generated by the fixed MM or QM particles on the polarizable sites, and $\boldsymbol{T}(\boldsymbol{\alpha})$ is the interaction matrix between the induced dipoles. The only parameter that is necessary for the ID model is the isotropic atomic polarizability for each polarizable site ($\boldsymbol{\alpha}$), which enters the diagonal elements of the $\boldsymbol{T}$ matrix. Minimizing the polarization energy with respect to the induced dipole leads to the equation to compute $\vec{\boldsymbol{\mu}}$:

$$\frac{\partial E^{Pol}}{\partial\vec{\boldsymbol{\mu}}}=\mathbf{T}(\boldsymbol{\alpha})\vec{\boldsymbol{\mu}}-\vec{\mathbf{E}}^{MM}-\vec{\mathbf{E}}^{QM}(\gamma)=0 \tag{54}$$

The expression in Equation 54 is the ID model equivalent of the PCM expression in Equation 6. Substituting Equation 54 into Equation 53, we obtain:

$$E^{Pol}=-\frac{1}{2}\vec{\boldsymbol{\mu}}\cdot\left[\vec{\mathbf{E}}^{MM}+\vec{\mathbf{E}}^{QM}(\gamma)\right]=-\frac{1}{2}\vec{\boldsymbol{\mu}}\cdot\vec{\mathbf{E}} \tag{55}$$

The form of the polarization energy in Equation 55 is equivalent to that for PCM in Equation 7. The difference is that the potential $\mathbf{V}$ and the charges $\mathbf{Q}$ are vectors of dimension equal to the number of finite elements into which the PCM cavity is discretized, while the electric field $\vec{\mathbf{E}}$ and dipole $\vec{\boldsymbol{\mu}}$ are $3\times N_{pol}$ matrices, where N_{pol} is the number of

polarizable sites. However, the operators corresponding to these energy terms are both one-electron operators, and the number and location of the charges/induced dipole sites disappears in the contraction of the electrostatic potential with the charges for PCM, and of the electric field with the induced dipoles in the ID model. In other words, these "environment" operators have the same functional form in terms of the interfacing with the CC equations. Thus, the entire theoretical framework (and corresponding code) derived for CC-PCM can be almost directly transferred to CC-MMpol. The only main difference between the two theories is that MMPol does not require a different treatment of fast processes, that is, the nonequilibrium solvation, because in vertical transitions the environment can be kept fixed at the equilibrium configuration. Although the equilibrium CC-PCM and CC-MMPol equations are essentially the same for both ground and excited states, it is important to remember that while in PCM the environment reorganization is implicit in the dielectric constant, in explicit models such reorganization must be obtained through a proper conformation sampling, for example, via a classical molecular dynamics (MD) simulation. Typically, a certain number of snapshots are extracted from the MD run, the QM-MMPol calculation is repeated for each snapshot, and the results are averaged out. In the context of CC-MMPol, this means that one needs to perform tens or hundreds of CC calculations, significantly increasing the computational effort compared to the in vacuo CC and CC-PCM cases. Additionally, if one were to use the full PTED scheme, this would increase the cost of each CC calculation for each snapshot but a factor of 3–5 (in our experience). Thus, the PTES approximation for the environment response becomes paramount in order to include the effect of the embedding explicitly in the CC equations without increasing the cost of each CC calculation compared to in vacuo CC. Despite the considerable computational cost of CC-MMPol compared to CC-PCM, there are cases where the former is necessary, for instance when the environment is not homogeneous (e.g., in a biomolecule) or when explicit solute-solvent interactions are important (e.g., H-bonding). In practice, the choice between implicit and explicit models depends on the compromise between computational cost and accuracy for a specific application.

3 | NUMERICAL APPLICATIONS

In this section, we present a number of applications of the CCSD-PCM-PTES method based on our implementation in the GAUSSIAN suite of programs.[64,65] These applications offer an initial assessment of the ability of the method to reproduce the data computed with the complete PTED scheme, and to model experimental data of molecules in solution, especially for excited states and response properties.

One of the first properties we studied is the solvation free energy for five small organic molecules in a variety of solvents.[44] In Table 1, we report the values computed in water for the PTED and PTES schemes and the corresponding experimental values. These calculations were performed with the 6–31 + G(d,p) basis set, the symmetric version of IEF-PCM,[58] and using UFF radii.[82] The geometries were optimized using the corresponding solvation scheme. The data in the table show that the calculations are in most cases less than 1 kcal/mol away from the experiment (1.4 kcal/mol for Cl-benzene), while the difference between PTES and PTED is 0.03–0.04 kcal/mol. At the same time, the number of iterations for the solution of the $\hat{T}$ amplitudes for CCSD-PCM-PTES is the same as that for the in vacuo calculations, that is, 16 iterations,[44] while for the PTED scheme the convergence of the PCM macroiteration is shown in Figure 1. The figure indicates that four PCM macro-iterations are necessary to reach an essentially converged value of the energy, for a total of about 90 iterations (adding the iterations for the $\hat{T}$ and $\hat{\Lambda}$ equations), i.e., about 5 times the number necessary for the PTES scheme.

The PTE scheme, which completely neglects any correlation contribution from the solvent, can be good enough to describe the ground state of small organic molecules, but we showed that the accuracy of the results deteriorates with the size of the system.[44] This is shown in Figure 2, where we consider a Fe complex used for hydrogen storage, and we report the solvation free energy in tetrahydrofuran (THF) as a function of the H—H bond length. The figure shows that

TABLE 1 Solvation free energy (kcal/mol) for five organic molecules in water. Experimental data (Exp) are taken from Reference 81, the calculated data are taken from References 42, 44

	Exp	PTED	PTES
Pyridine	−4.70	−4.80	−4.77
Aniline	−5.49	−5.38	−5.35
Phenol	−6.62	−5.85	−5.82
p-Br-phenol	−7.13	−6.36	−6.33
Cl-benzene	−1.12	−2.57	−2.53

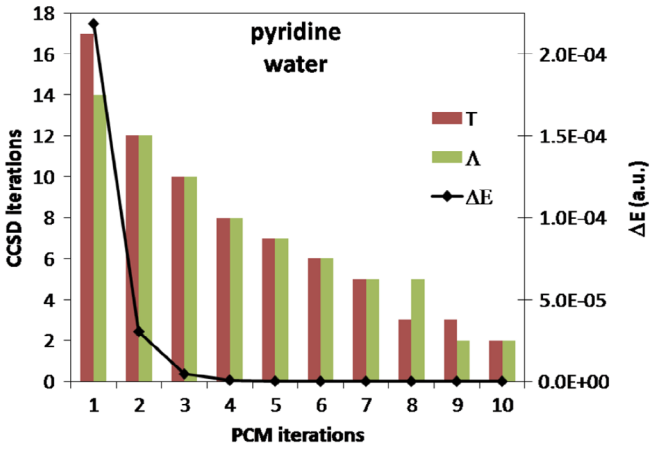

FIGURE 1 Convergence of the CCSD-PTED-PCM equations for the calculation of the solvation free energy (kcal/mol) of pyridine in water. Reproduced with permission from Reference 42. Copyright 2010 American Chemical Society

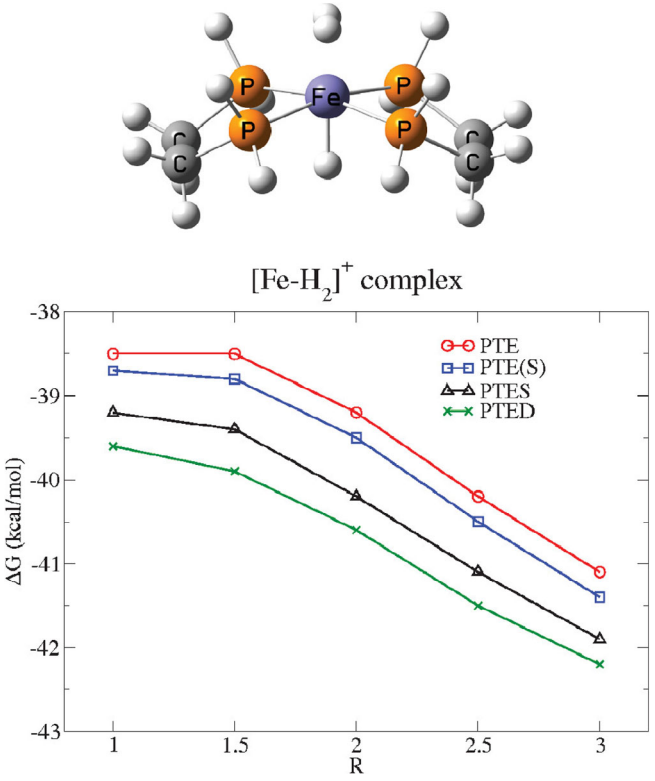

FIGURE 2 Solvation free energy (kcal/mol) for the H_2[FeH$(PP)_2$] + complex in THF at various H–H bond distances. R is a scaling factor from the equilibrium bond distance. Reproduced with permission from Reference 44. Copyright 2011 AIP Publishing

the PTE scheme misses up to 1.5 kcal/mol in ΔG compared with PTED, while the PTES scheme recovers over 70% of this difference without increasing the computational cost of the calculation compared to PTE.

In Reference 45, we studied the vertical absorption and emission energies computed with the SS formalism for two small organic molecules: acrolein and methylcyclopropene (MCP). Experimental data are available for absorption, and they are reported in Tables 2, 3.

The calculated data used the solvent model with dispersion (SMD),[81] which is IEF-PCM for the electrostatic part, and a series of models for nonelectrostatic interactions. The latter are introduced as classical terms, therefore, they do not enter the CC equations, but they do affect the optimized molecular geometry (similar to the nuclear-nuclear repulsion energy). SMD also has its own set of cavity radii.[81] The calculations in solution reproduce the solvatochromic red and blue shifts of the excitation energies compared to gas phase and between solvents. The absolute errors on the excitation energies tend to be larger in solution than in gas phase, which is not surprising giving the approximate nature of PCM. Nevertheless, the solvent shift are almost quantitatively reproduced for acrolein; for MCP, half of the shift is recovered for the first transition, while for the second transition the difference between solvents is small, and a

continuum model alone is not sufficient to distinguish their effect. In general, PTES performs slightly better than PTED, probably because in the latter the $\hat{T}$ amplitudes are computed in the presence of the excited state charges $\mathbf{Q}_{KN}$, due to the coupling of all amplitude equations introduced by the solvent term, see Equation 21. Using the PTE approximation for vertical absorption energies leads to values that are 0.05–0.13 eV higher than with the PTES scheme for acrolein, and 0.04–0.32 eV for MCP, worsening the agreement with experiment.[45] These differences are even more severe for vertical emission energies, as shown in Tables 4, 5, where the PTED optimized geometry is used to focus on the electronic effects only.

Although no experimental data are available for a quantitative comparison, the PTED and PTES schemes provide the same qualitative picture, that is, a negative shift of the emission energy passing from a nonpolar to a polar solvent. On the other hand, the PTE scheme (referred to as frozen reaction field, FRF, in Reference 45) provides a positive shift. This is an example of how important solvent effects can be for excited states, such that including them only in the reference wave function may provide qualitatively incorrect trends.

We also performed a benchmark study of excitation energies for larger systems computed with the PTED-LR scheme, shown in Figure 3.[51] The highlights of that study are that the error of CC-PCM calculations on transition energies is typically of the order of 0.4–0.5 eV, therefore somewhat larger than for in vacuo calculations.[83] This is again to

TABLE 2 Vertical excitation energies (eV) in gas and in solution phase for the first two transitions of acrolein. The solvent shift is the excitation energy difference between the polar and nonpolar solvent[45]

	$n \rightarrow \pi^* \; A''$				$\pi \rightarrow \pi^* \; A'$			
	Exp	**PTED**	**PTES**	**PTE**	**Exp**	**PTED**	**PTES**	**PTE**
Gas	3.71	3.88	3.88	3.88	6.41	6.80	6.80	6.80
Cyclohexane	3.71	3.87	3.84	3.93	6.11	6.71	6.69	6.76
Water	3.94	4.05	4.03	4.18	5.90	6.54	6.49	6.56
Solvent shift	+0.23	+0.18	+0.19	+0.25	−0.21	−0.17	−0.20	−0.20

TABLE 3 Vertical excitation energies (eV) in gas and in solution phase for the first two transitions of MCP. The solvent shift is the excitation energy difference between the polar and nonpolar solvent[45]

	$\pi \rightarrow \pi^* \; B_2$				$\pi \rightarrow \pi^* \; A_1$			
	Exp	**PTED**	**PTES**	**PTE**	**Exp**	**PTED**	**PTES**	**PTE**
Gas		4.48	4.48	4.48		6.15	6.15	6.15
n-pentane	4.01	4.43	4.32	4.62	6.02	6.10	6.09	6.15
Methanol	4.49	4.64	4.57	4.89	5.90	6.10	6.10	6.14
Solvent shift	+0.48	+0.21	+0.25	+0.27	−0.12	0.00	+0.01	−0.02

TABLE 4 Vertical emission energies (eV) in gas and in solution phase for acrolein computed at the PTED optimized geometry[45]

	$\pi^* \rightarrow n \; A''$		
	PTED	**PTES**	**PTE**
Cyclohexane	3.17	3.11	3.24
Water	3.02	2.76	3.77
Solvent shift	−0.15	−0.35	+0.43

TABLE 5 Vertical emission energies (eV) in gas and in solution phase for MCP computed at the PTED optimized geometry[45]

	$\pi^* \rightarrow \pi \; B$		
	PTED	**PTES**	**PTE**
n-pentane	1.43	1.30	1.64
Methanol	1.09	0.76	2.07
Solvent shift	−0.34	−0.54	+0.43

be expected, as standard PCM does not account for nonelectrostatic effects in the excitation process, and for specific solute-solvent interactions. However, the study in Reference 51 also showed that the effect of H-bonding, one of the main issues with PCM, can be recovered at a cheaper level of theory. In particular, we created microsolvated clusters with a few explicit solvent molecules H-bonded to the solute, and surrounded the cluster with a continuum dielectric. We showed that an energy correction, computed as the difference between the excitation energy for the micro-solvated cluster-PCM and for the PCM-only calculations evaluated at TD-DFT level, can substantially improve the agreement of CC-PCM with experiment. Additionally, this correction is not very sensitive to the choice of approximate density functional, contrary to the actual value of the excitation energy.[83] In a follow-up study,[52] we performed similar calculations on the same molecules in Figure 3 with the PTES-LR scheme. The relative error with respect to the PTED scheme for the transition energy as well as for the oscillator strength computed with the full LR approach (see Equations 40–43) and with the approximate EOM approach[69] (f-si and f-nsi, respectively) are shown in Figure 4. The plots in the figure show that the PTES and PTED results are essentially identical (the larger error bars for the oscillator strengths are due to f values that are small in magnitude, which lead to misleadingly large relative errors). However, there is a significant difference in the computational cost to solve the CC equations for the various sets of amplitudes between the two schemes, detailed in Table 6. The table shows that the solution of the ground state equations is four times faster with PTES compared with PTED. On the other hand, the excited state amplitudes require the same computational effort, because a PTES-type approximation is invoked in the PTED-LR scheme, as discussed in Section 2.2.2.[12,28,52] In the same work, we also computed the specific rotation for three organic molecules. The sign of the specific rotation is directly

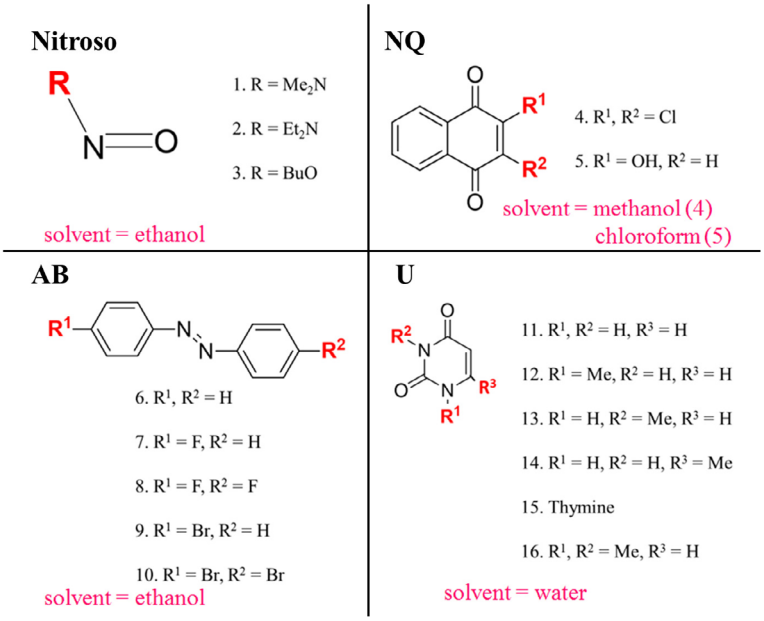

FIGURE 3 Test set used for the benchmarking of LR-CCSD-PCM against experiment. This includes 16 molecules divided in four groups: Nitroso, NQ, AB, and U, and the solvents in which measurements were performed. Reproduced with permission from Reference 51. Copyright 2017 American Chemical Society

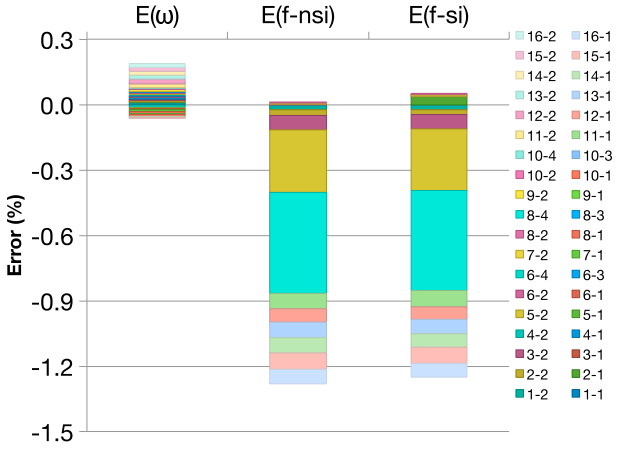

FIGURE 4 Cumulative, signed relative error (%) of PTES-LR compared to PTED-LR for the excitation energy (E[ω]), the oscillator strength with the nonsize intensive (E[f-nsi]) and with the size intensive approaches (E[f-si]) for the 16 molecules of Reference 51; the label x-y indicates state y of molecule x (as in Reference 51). Reproduced with permission from Reference 52. Copyright 2018 AIP Publishing

TABLE 6 Total number of iterations to solve the $\hat{T}$, $\hat{\Lambda}$, $\hat{R}_K$, $\hat{L}_K$, and $\hat{M}_K$ amplitudes equations with CCSD-PTES-LR for the 16 molecules from Reference 51. The total sum (Tot) and the sum without the $\hat{M}_K$ iterations (Tot – N_M) are also reported[52]

	PTED	PTES
$\hat{T}$	1,135	291
$\hat{\Lambda}$	1,118	299
$\hat{R}_K$	984	980
$\hat{L}_K$	674	677
$\hat{M}_K$	412	412
Tot	4,323	2,659
Tot – N_M	3,911	2,247

TABLE 7 Specific rotation (deg dm^{-1} $[g/ml]^{-1}$) for (1R,3R,5R,7R)-bisnoradamantan-2-one (**1**) in ethanol, (1R,5S)-nopinone (**2**) in methanol, and (1S,4R)-norbornanone (**3**) in chloroform. MVG: Modified velocity gauge; LG: length gauge[52]

		MVG		LG	
	Exp	Gas	PTES	Gas	PTES
1	−78.4	50.3	−7.7	19.8	−26.0
2	39.9	−8.4	41.4	−8.0	36.4
3	29.8	5.0	4.2	−7.9	1.4

related to the absolute configuration of a nonracemic sample of a chiral compound. Therefore, obtaining the correct sign of this electronic property is essential for a meaningful comparison with experiment. In certain cases, the solvent is able to change the sign of the specific rotation compared to that of an enantiomer in the gas phase. Thus, taking into account solvation effects is paramount. Table 7 reports three cases that exemplify the importance of solvation effects,[52,84] where the specific rotation calculated in the gas phase and in solution have the opposite sign (the values computed with PTED are basically the same as those with PTES, and they are not reported). However, we should caution that, in most cases, a treatment of the solvation effects based only on a polarizable classical model is likely not enough to reproduce experimental trends,[85] and a QM treatment of the first solvation shell may be necessary.

The implementation of the excited state energy gradients for the PTES-LR scheme at the CCSD level allowed us to explore the PES of larger systems than possible with the SS approach.[54] In particular, we focused on 4-(N,N)-dimethylaminobenzonitrile (DMABN), because this molecule shows dual fluorescence in polar solvents, but not in gas phase and in nonpolar solvents.[86–93] The dual fluorescence derives from a locally excited state (LE), and a twisted intramolecular charge-transfer state (TICT) that is stabilized only in polar solvents, see Figure 5 for a representation of the optimized geometries of the ground state (GS), and of the LE and CT states. The plots of the energies of these three states (relative to the GS minimum energy in gas phase) are shown in Figures 6–8. The plots in Figure 6 show the correct order of the states in the gas phase calculations, that is, the LE state is lower in energy than the CT state, in agreement with the observation that only one emission band is present. However, the data in cyclohexane and acetonitrile show some of the limitations of the SS and LR formalisms, see Figures 7 and 8. In particular, the LR formalism reproduces the correct state order in cyclohexane (LE more stable than CT), but not in acetonitrile (LE still more stable than CT). In contrast, the SS formalism provides the complete opposite prediction: the CT state is more stable than the LE state in both solvents, where experimentally this is observed only for acetonitrile. The reason why the LR formalism is not able to stabilize enough the CT state in acetonitrile is that the solvent response can be related to the magnitude of the transition dipole,[67,68] which is small in the twisted structure (see Figure 5) because the conjugation across the entire molecule is broken. On the other hand, the solvent response in the SS formalism is related to the state dipole, which is large in the CT state because of the charge separation. However, the SS formalism tends to overestimate this effect, thus stabilizing the CT state too much in cyclohexane. It was shown that both formalisms account for a particular type of solute-solvent interaction: the SS formalisms account for the mutual polarization between the molecule and the environment, while the LR formalism accounts for dispersive interactions.[67,68,94] Hence, it has been suggested that two can be combined as[90,95]:

$$\Delta E = \omega_0 + \Delta\Delta E_{LR} + \Delta\Delta E_{SS} \tag{56}$$

where ω_0 is the transition energy computed with the frozen ground state reaction field ($\mathbf{Q}^0 + \mathbf{Q}_N^T$), and

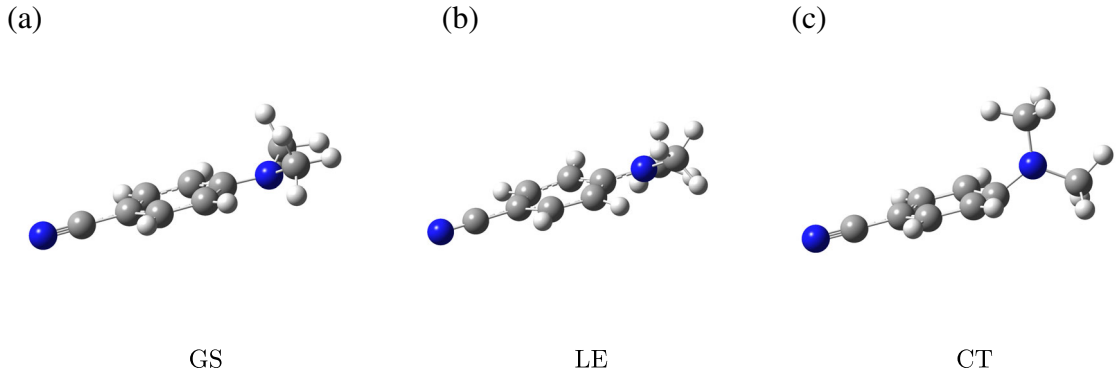

FIGURE 5 Optimized geometry of DMABN in the ground state (a), the LE state (b), and the CT state (c) in the gas phase. The optimized structures in solution are similar. Reproduced with permission from Reference 54. Copyright 2019 Wiley-VCH Verlag GmbH & Co. KGaA

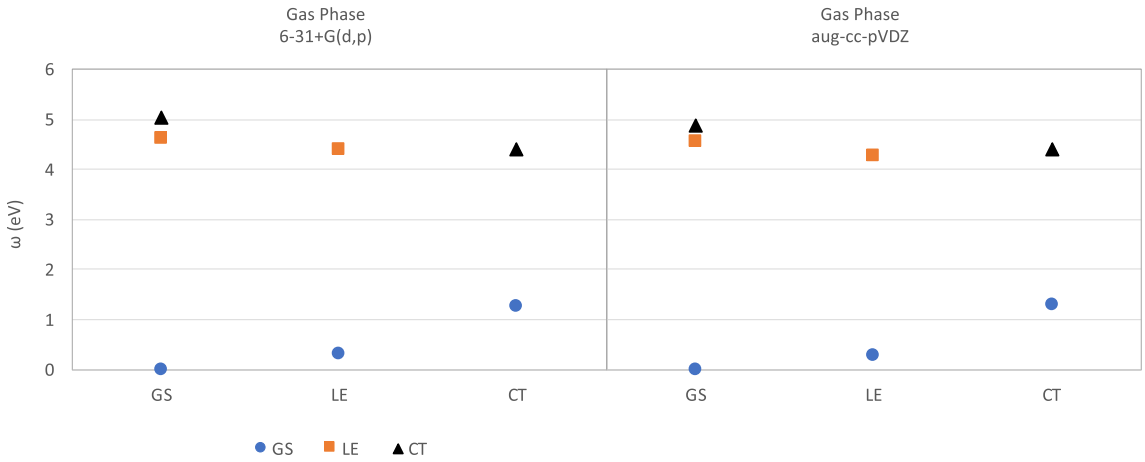

FIGURE 6 Relative energy (eV) of the GS, LE, and CT electronic states of DMABN at the various optimized geometries in the gas phase. The reference energy is the minimum GS energy. The x axis reports the electronic state for which the geometry was optimized. Reproduced with permission from Reference 54. Copyright 2019 Wiley-VCH Verlag GmbH & Co. KGaA

$$\begin{aligned} \Delta\Delta E_{LR} = &\ \Delta E_{LR} - \omega_0 \\ \Delta\Delta E_{SS} = &\ \Delta E_{SS} - \omega_0 \end{aligned} \tag{57}$$

where $\Delta E_{SS/LR}$ are the excitation energies computed with the SS and LR formalisms, respectively, as discussed in Sections 2.2.1–2.2.2. Vertical excitation energies are reported for DMABN in the two solvents and for the two states in Tables 8, 9. The results in the tables confirm that CCSD-PCM tends to overestimate the experimental absorption energies, especially when only the ground state solvation effects are included (ω_0 data). The combination of the LR and SS formalism as in Equation 56 moves the excitation energy closer to the experimental value compared to both approaches. However, this improvement is rather small in most cases (below 0.1 eV) compared to the difference with experiment. The state energies at the excited state equilibrium geometries (relative to GS gas phase minimum energy) are reported in Tables 10, 11. The data in the tables show that the SS-LR combination moves the calculated values in the right direction, in the sense that it reduces the difference in energy between the LE and CT states, thus reducing the difference in emission energies computed with the SS approach in Reference 54. However, this approach is still not able to reproduce the correct energy order in cyclohexane, and the CT state is 0.2 eV lower in energy than the LE state with the 6–31 + G(d,p) basis set, and 0.1 eV with the aug-cc-pVDZ basis set. Given the decreasing gap with increasing basis set size, it is possible that the incorrect energy order is due to the limitation in the number of basis functions used in these calculations.

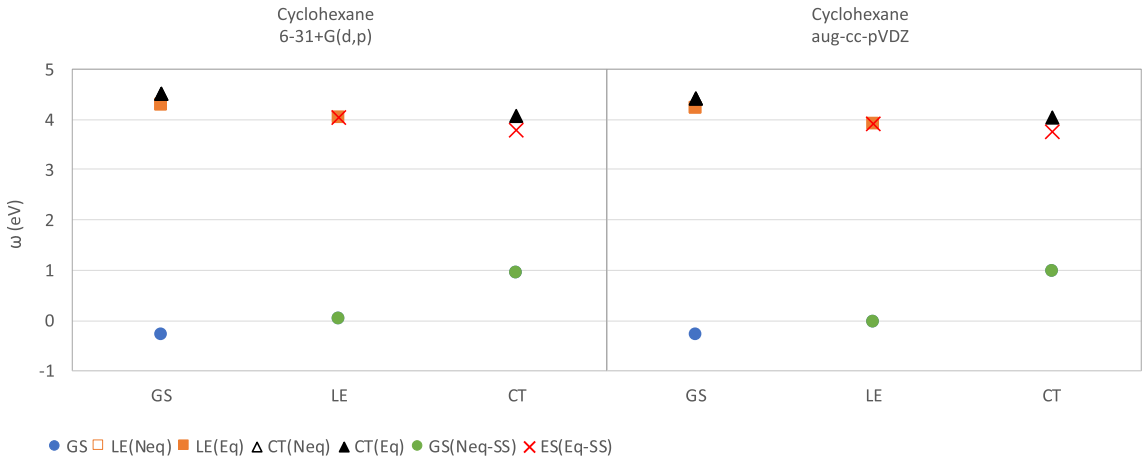

FIGURE 7 Relative energy (eV) of the GS, LE, and CT electronic states of DMABN at the various optimized geometries in cyclohexane solution. The reference energy is the minimum GS energy in the gas phase. The x axis reports the electronic state for which the geometry was optimized. The labels Eq and Neq refer to the equilibrium and nonequilibrium solvation regimes, respectively. All calculations are performed with the LR formalism except those with the SS label, where ES stands for excited state. Reproduced with permission from Reference 54. Copyright 2019 Wiley-VCH Verlag GmbH & Co. KGaA

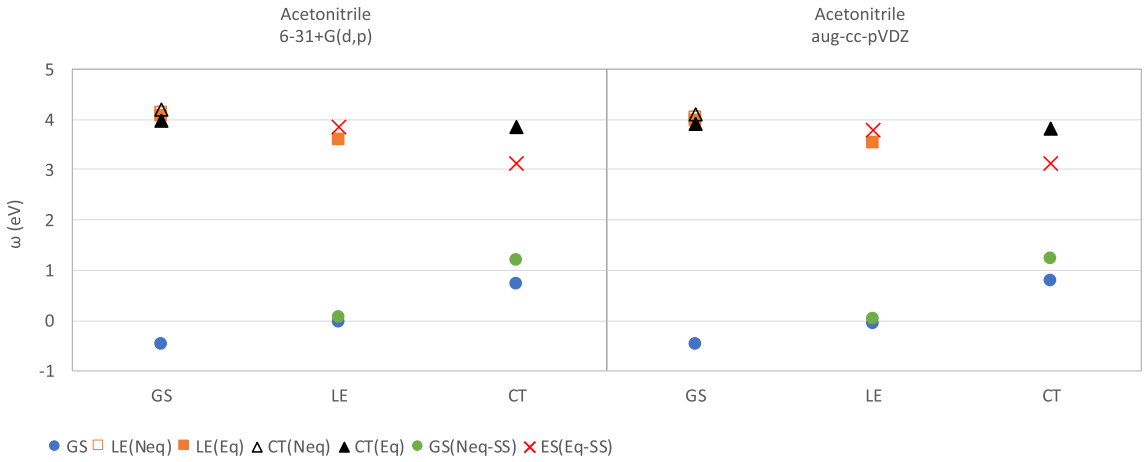

FIGURE 8 Relative energy (eV) of the GS, LE, and CT electronic states of DMABN at the various optimized geometries in acetonitrile solution. The reference energy is the minimum GS energy in the gas phase. The x axis reports the electronic state for which the geometry was optimized. The labels Eq and Neq refer to the equilibrium and nonequilibrium solvation regime, respectively. All calculations are performed with the LR formalism except those with the SS label, where ES stands for excited state. Reproduced with permission from Reference 54. Copyright 2019 Wiley-VCH Verlag GmbH & Co. KGaA

TABLE 8 Vertical excitation energies (eV) for DMABN in cyclohexane

	6–31 + G(d,p)		Aug-cc-pVDZ	
	LE	CT	LE	CT
Exp	4.05	4.47	4.05	4.47
ω_0	4.63	4.94	4.54	4.82
ΔE_{LR}	4.60	4.80	4.51	4.70
ΔE_{SS}	4.59	4.87	4.50	4.77
ΔE	4.56	4.73	4.47	4.65

A final application that we wish to discuss is the comparison of the CCSD-MMPol method with full CCSD for the calculation of vertical excitation energies in microsolvated clusters.[53] We considered three small/medium organic molecules: formaldehyde, acrolein, and diazobenzene surrounded by 2–6 water molecules, or 2 chloroform molecules. These

	6–31 + G(d,p)		Aug-cc-pVDZ	
	LE	CT	LE	CT
Exp	3.86	4.21	3.86	4.21
ω_0	4.64	4.81	4.55	4.71
ΔE_{LR}	4.60	4.68	4.51	4.59
ΔE_{SS}	4.60	4.73	4.51	4.65
ΔE	4.56	4.60	4.47	4.53

TABLE 9 Vertical excitation energies (eV) for DMABN in acetonitrile

	6–31 + G(d,p)		Aug-cc-pVDZ	
	LE	CT	LE	CT
ω_0	4.10	4.07	3.97	4.05
ΔE_{LR}	4.05	4.07	3.92	4.05
ΔE_{SS}	4.04	3.78	3.92	3.77
ΔE	3.99	3.79	3.87	3.77

TABLE 10 State energies (eV) at the corresponding excited state equilibrium geometry for DMABN in cyclohexane. The zero of the energy is taken at the GS minimum energy in the gas phase

	6–31 + G(d,p)		Aug-cc-pVDZ	
	LE	CT	LE	CT
ω_0	3.99	3.83	3.91	3.81
ΔE_{LR}	3.61	3.84	3.55	3.82
ΔE_{SS}	3.86	3.12	3.79	3.11
ΔE	3.48	3.14	3.43	3.12

TABLE 11 State energies (eV) at the corresponding excited state equilibrium geometry for DMABN in acetonitrile. The zero of the energy is taken at the GS minimum energy in the gas phase

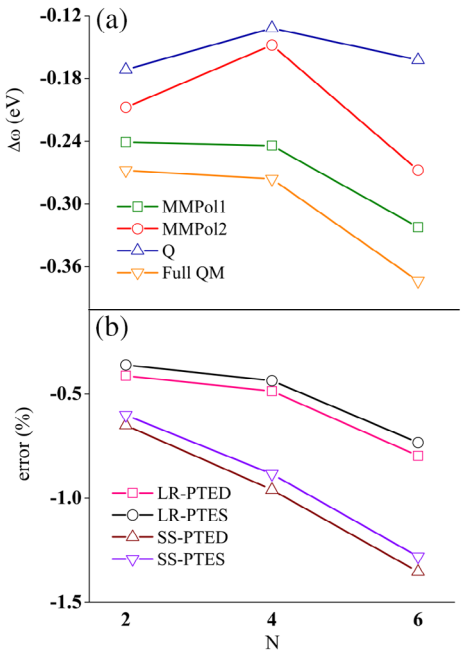

FIGURE 9 Panel a: solvatochromic shifts in the excitation energies of acrolein with two to six water molecules (N) computed at EOM-CCSD/aug-cc-pVDZ level. Panel b: corresponding relative errors for the four EOM-CCSD/MMPol1 schemes. For the gas phase solute $\omega = 6.8$ eV and $f = 0.29$. Reproduced with permission from Reference 53. Copyright 2019 American Chemical Society

clusters were small enough to be treatable with the full EOM-CCSD method. We did a thorough test of six basis sets, two choices of polarizable environment (either with three induced dipoles centered on each atom, or one induced dipole centered on the oxygen of the water molecule), and a nonpolarizable force field (i.e., only fixed point charges).

The results showed that the aug-cc-pVDZ basis set is a good compromise between computational cost and accuracy, and that the model with induced dipoles on each atom of the environment is necessary to obtain accurate results. These trends are exemplified in Figure 9, which shows the change in excitation energy for acrolein by increasing the number of solvating water molecules. With these choices, the relative errors compared to the full EOM-CCSD calculations are around 0–2% across the entire test set. There is not a significant preference between the SS and LR formalisms, as they alternate for the best agreement with the full CC calculations. We found no appreciable difference between the PTED and PTES schemes. Hence, we recommended the PTES-LR scheme as the best compromise between computational effort and accuracy.[53]

4 | CONCLUSIONS

In this work, we have reviewed how to combine CC methods with PCM, using the singles-T density approximation for the correlation solvent effect, called PTES scheme. This scheme was introduced to avoid the coupling of the $\hat{T}$ and $\hat{\Lambda}$ amplitude equations in the ground state, and with $\hat{R}_K$ and $\hat{L}_K$ in the excited state. The name "singles-T" comes from the fact that the PCM charges are computed with an approximate reduced 1PDM, formed from the single excitation $\hat{T}$ amplitudes. However, the expression "singles-T" does not refer to the level of truncation chosen for the CC wave function. In fact, although our implementation of the CC-PCM method is limited to CCSD, the equations presented in this review are general, and can be applied to higher levels of truncation. We have also discussed how the PCM-PTES scheme changes the $\hat{\Lambda}$ equations and the energy gradients, such that geometry optimizations and ground state properties calculations (such as the dipole moment) can be performed for solvated molecules at CC level. We then introduced the theory for excited states in the SS and LR formalisms. The former is based on the response of the solvent to the excited state density of the solute, while in the latter the solvent responds to the transition density. It was shown that the SS formalism reproduces the mutual electrostatic polarization interaction between solute and solvent, while the LR formalism models dispersion interactions.[67,68,94] For both formalisms, we presented the equations for the energy and for the energy gradients. For LR, we also presented the equations for the evaluation of linear response properties, such as the electric polarizability or the specific rotation. Finally, we have shown how the same theoretical framework can be applied to polarizable force fields, specifically those based on the induced dipole model, in a way that is transparent to the CC equations.

For all these cases, we discussed the extra computational cost due to the PTES scheme, which scales at most as $O(N^5)$, because this is the scaling to evaluate the various forms of the 1PDMs necessary in ground and excited state calculations. Since CCSD scales as $O(N^6)$, the CCSD-PCM-PTES method costs the same as in vacuo CCSD. The only exception is the SS formalism for the evaluation of the excited state energy, because the solvent couples the $\hat{R}_K$ and $\hat{L}_K$ amplitude equations. Nevertheless, this is computationally cheaper and possibly better defined than the full PTED scheme, where the equations for the $\hat{T}$, $\hat{\Lambda}$ k, $\hat{R}_K$, and $\hat{L}_K$ amplitudes are all coupled, and the $\hat{T}$ amplitudes are computed in the presence of the excited state PCM charges. Even for the LR formalism, the PTES scheme is better defined than the PTED scheme, because in the latter the solvent would couple the equations for the perturbed $\hat{T}$ and $\hat{\Lambda}$ amplitudes. This coupling is usually neglected in the LR response part of the calculation,[12,28,52] creating an inconsistency in the level of approximation for the energy and the corresponding linear response function. Such inconsistency is avoided in the PTES scheme, because the $\hat{T}/\hat{\Lambda}$ coupling is removed in the energy expression, and the amplitudes equations are naturally decoupled in the LR function. Overall, the CC-PCM-PTES-LR method is virtually identical in cost to in vacuo LR-CC.

In Section 3, we discussed a series of applications of the methods detailed in Section 2. These applications targeted comparisons with experimental data, and internal comparisons between the PTED and PTES schemes, for both ground and excited state properties. We showed that the PTES scheme provides results that are very close to those of PTED, at a fraction of the computational cost. We also showed that neglecting the contributions of the solvent in the CC equations (i.e., the PTE scheme) reduces the agreement with experiment, see Tables 2, 3, or it can lead to wrong qualitative trends, see Tables 4, 5. Solvation effects are also important for molecular properties, like the specific rotation in Table 7. We employed the excited state energy gradients for the PTES-LR scheme to study the absorption and emission spectra of DMABN, which shows dual fluorescence in polar solvents. This example allowed us to outline some limitations of the LR and SS formalisms in implicit models. In particular, the LR underestimates the stabilization of the CT state in polar solvents, while the SS formalism overestimates it, so that each formalism gets the order of the states wrong in either the polar or the nonpolar solvents, see Figures 7 and 8. Combining the two effects as a single correction to the

excitation energy computed with the solvent reaction field of the ground state improves the results, but this is not enough to recover the correct experimental trends. This is probably due to intrinsic limitations of implicit solvation models, where nonelectrostatic interactions and direct solute-solvent interactions are difficult to mimic. A combined approach, where the H-bonding effect computed with a lower and less demanding level of theory (e.g., DFT) are introduced as a correction to the CC-PCM energies, may help to overcome these limitations, and improve the agreement with experiment.[51] Alternatively, one can employ explicit polarizable force fields, using the same approximate schemes devised for PCM. In fact, we showed that the MMPol-PTES scheme can reproduce the same trends of transition energies computed with full EOM-CCSD for a series of microsolvated organic molecules, see Figure 9 and Reference 53.

Despite some of their limitations, PCM and other implicit solvation models are a fast and reliable way to account for solvent effects in correlation calculations. In particular, the CC-PCM-PTES scheme has the same computational cost as in vacuo CC, and it has the potential to become as widely used as DFT-PCM for studying solvated molecules. The CC-PCM combination is not limited in principle to only ground state and linear response calculations, and we are currently working to extend it to higher order properties.

ACKNOWLEDGMENTS

We wish to thank Dr. Giovanni Scalmani (Gaussian, Inc.) for help in the implementaion of PCM code, and Ms. Sijin Ren (University of Kansas) for the development of the CCSD-MMPol method. This work has been partially supported by the National Science Foundation under the grant CHE-1650942.

ORCID


Marco Caricato https://orcid.org/0000-0001-7830-0562

RELATED WIRES ARTICLES

Single-reference coupled cluster methods for computing excitation energies in large molecules: The efficiency and accuracy of approximations

REFERENCES

1. Warshel A, Levitt M. Theoretical studies of enzymic reactions: Dielectric, electrostatic and steric stabilization of the carbonium ion in the reaction of lysozyme. *J Mol Biol*. 1976;*103*(2):227–249.
2. Lin H, Truhlar D. QM/MM: What have we learned, where are we, and where do we go from here? *Theor Chem Acc*. 2007;*117*(2):185–199.
3. Senn HM, Thiel W. QM/MM methods for biomolecular systems. *Angew Chem Int Ed*. 2009;*48*(7):1198–1229.
4. Tomasi J, Mennucci B, Cammi R. Quantum mechanical continuum solvation models. *Chem Rev*. 2005;*105*(8):2999–3093.
5. Mennucci B, Cammi R, editors. *Continuum Solvation models in chemical physics*. Chichester: Wiley-Blackwell, 2007.
6. Mennucci B. Continuum solvation models: What Else can W e learn from them? *J Phys Chem Lett*. 2010;*1*:1666–1674.
7. Bartlett RJ, Musial M. Coupled-cluster theory in quantum chemistry. *Rev Mod Phys*. 2007;*79*(1):291–352.
8. Shavitt I, Bartlett RJ. *Many-body methods in chemistry and physics*. Cambridge: Cambridge University Press, 2009.
9. del Valle FJO, Tomasi J. Electron correlation and solvation effects. I. Basic formulation and preliminary attempt to include the electron correlation in the quantum mechanical polarizable continuum model so as to study solvation phenomena. *Chem Phys*. 1991;*150*(2):139–150.
10. Aguilar MA, del Valle FJO, Tomasi J. Electron correlation and solvation effects. II. The description of the vibrational properties of a water molecule in a dielectric given by the application of the polarizable continuum model with inclusion of correlation effects. *Chem Phys*. 1991;*150*(2):151–161.
11. Christiansen O, Mikkelsen KV. A coupled-cluster solvent reaction field method. *J Chem Phys*. 1999;*110*(3):1365–1375.
12. Christiansen O, Mikkelsen KV. Coupled cluster response theory for solvated molecules in equilibrium and nonequilibrium solvation. *J Chem Phys*. 1999;*110*(17):8348–8360.
13. Christiansen O, Jorgensen P, Hattig C. Response functions from Fourier component variational perturbation theory applied to a time-averaged quasienergy. *Int J Quantum Chem*. 1998;*68*(1):1–52.
14. Kongsted J, Osted A, Mikkelsen KV, Christiansen O. The QM/MM approach for wavefunctions, energies and response functions within self-consistent field and coupled cluster theories. *Mol Phys*. 2002;*100*(11):1813–1828.
15. Kongsted J, Osted A, Mikkelsen KV, Christiansen O. Nonlinear optical response properties of molecules in condensed phases using the coupled cluster/dielectric continuum or molecular mechanics methods. *J Chem Phys*. 2003;*119*(20):10519–10535.
16. Kongsted J, Osted A, Mikkelsen KV, Christiansen O. Linear response functions for coupled cluster/molecular mechanics including polarization interactions. *J Chem Phys*. 2003;*118*(4):1620–1633.
17. Osted A, Kongsted J, Mikkelsen KV, Christiansen O. A CC2 dielectric continuum model and a CC2 molecular mechanics model. *Mol Phys*. 2003;*101*(13):2055–2071.

18. Kongsted J, Osted A, Mikkelsen KV, Christiansen O. Molecular electric properties of liquid water calculated using the combined coupled cluster/molecular mechanics method. *J Mol Struct THEOCHEM*. 2003;*632*(1):207–225.
19. Sneskov K, Schwabe T, Kongsted J, Christiansen O. The polarizable embedding coupled cluster method. *J Chem Phys*. 2011;*134*(10): 104108.
20. Nielsen CB, Christiansen O, Mikkelsen KV, Kongsted J. Density functional self-consistent quantum mechanics/molecular mechanics theory for linear and nonlinear molecular properties: Applications to solvated water and formaldehyde. *J Chem Phys*. 2007;*126*(15): 154112.
21. Steindal AH, Ruud K, Frediani L, Aidas K, Kongsted J. Excitation energies in solution: The fully polarizable QM/MM/PCM method. *J Phys Chem B*. 2011;*115*(12):3027–3037.
22. Olsen JMH, Steinmann C, Ruud K, Kongsted J. Polarizable density embedding: A new QM/QM/MM-based computational strategy. *J Phys Chem A*. 2015;*119*(21):5344–5355.
23. Olsen JM, Aidas K, Kongsted J. Excited states in solution through polarizable embedding. *J Chem Theory Comput*. 2010;*6*(12):3721–3734.
24. Curutchet C, Muñoz-Losa A, Monti S, Kongsted J, Scholes GD, Mennucci B. Electronic energy transfer in condensed phase studied by a polarizable QM/MM model. *J Chem Theory Comput*. 2009;*5*(7):1838–1848.
25. List NH, Olsen JMH, Kongsted J. Excited states in large molecular systems through polarizable embedding. *Phys Chem Chem Phys*. 2016;*18*:20234–20250.
26. Cammi R. Quantum cluster theory for the polarizable continuum model. I. the CCSD level with analytical first and second derivatives. *J Chem Phys*. 2009;*131*(16):164104.
27. Cammi R. Coupled-cluster theories for the polarizable continuum model. II. Analytical gradients for excited states of molecular solutes by the equation of motion coupled-cluster method. *Int J Quantum Chem*. 2010;*110*(15):3040–3052.
28. Cammi R. Coupled-cluster theory for the polarizable continuum model. III. A response theory for molecules in solution. *Int J Quantum Chem*. 2012;*112*(13):2547–2560.
29. Cammi R, Fukuda R, Ehara M, Nakatsuji H. Symmetry-adapted cluster and symmetry-adapted cluster-configuration interaction method in the polarizable continuum model: Theory of the solvent effect on the electronic excitation of molecules in solution. *J Chem Phys*. 2010;*133*(2):024104.
30. Fukuda R, Ehara M, Nakatsuji H, Cammi R. Nonequilibrium solvation for vertical photoemission and photoabsorption processes using the symmetry-adapted cluster–configuration interaction method in the polarizable continuum model. *J Chem Phys*. 2011;*134*(10):104109.
31. Fukuda R, Ehara M. Electronic excitation of molecules in solution calculated using the symmetry-adapted cluster–configuration interaction method in the polarizable continuum model. *AIP Conf Proc*. 2015;*1702*(1):090012.
32. Fukuda R, Ehara M, Cammi R. Modeling molecular Systems at Extreme Pressure by an extension of the polarizable continuum model (PCM) based on the symmetry-adapted cluster-configuration interaction (SAC–CI) method: Confined electronic excited states of furan as a test case. *J Chem Theory Comput*. 2015;*11*(5):2063–2076.
33. Fukuda R, Ehara M, Cammi R. Electronic excitation spectra of molecules in solution calculated using the symmetry-adapted cluster-configuration interaction method in the polarizable continuum model with perturbative approach. *J Chem Phys*. 2014;*140*(6):064114.
34. DeFusco A, Minezawa N, Slipchenko LV, Zahariev F, Gordon MS. Modeling solvent effects on electronic excited states. *J Phys Chem Lett*. 2011;*2*(17):2184–2192.
35. Ghosh D, Isayev O, Slipchenko LV, Krylov AI. Effect of solvation on the vertical ionization energy of thymine: From microhydration to bulk. *J Phys Chem A*. 2011 JUN 16;*115*(23):6028–6038.
36. Gordon MS, Fedorov DG, Pruitt SR, Slipchenko LV. Fragmentation methods: A route to accurate calculations on large systems. *Chem Rev*. 2012;*112*(1):632–672.
37. Hoffman GJ, Gurunathan PK, Francisco JS, Slipchenko LV. Excited states of OH-(H2O)(n) clusters for n=1-4: An ab initio study. *J Chem Phys*. 2014;*141*:104315.
38. Ghosh D, Kosenkov D, Vanovschi V, et al. Effective fragment potential method in Q-CHEM: A guide for users and developers. *J Comput Chem*. 2013;*34*(12):1060–1070.
39. Sadybekov A, Krylov AI. Coupled-cluster based approach for core-level states in condensed phase: Theory and application to different protonated forms of aqueous glycine. *J Chem Phys*. 2017;*147*(1):014107.
40. Ghosh D. Hybrid equation-of-motion coupled-cluster/effective fragment potential method: A route toward understanding Photoprocesses in the condensed phase. *J Phys Chem A*. 2017;*121*(4):741–752.
41. Howard JC, Womack JC, Dziedzic J, Skylaris CK, Pritchard BP, Crawford TD. Electronically excited states in solution via a smooth dielectric model combined with equation-of-motion coupled cluster theory. *J Chem Theory Comput*. 2017;*13*(11):5572–5581.
42. Caricato M, Scalmani G, Trucks GW, Frisch MJ. Coupled cluster calculations in solution with the polarizable continuum model of solvation. *J Phys Chem Lett*. 2010;*1*(15):2369–2373.
43. Caricato M, Scalmani G, Frisch MJ. Brueckner doubles coupled cluster method with the polarizable continuum model of solvation. *J Chem Phys*. 2011;*134*(24):244113.
44. Caricato M. CCSD-PCM: Improving upon the reference reaction field approximation at no cost. *J Chem Phys*. 2011;*135*(7):074113.
45. Caricato M. Absorption and emission spectra of solvated molecules with the EOM–CCSD–PCM method. *J Chem Theory Comput*. 2012;*8* (11):4494–4502.
46. Caricato M. Exploring potential energy surfaces of electronic excited states in solution with the EOM-CCSD-PCM method. *J Chem Theory Comput*. 2012;*8*(12):5081–5091.

47. Caricato M. Implementation of the CCSD-PCM linear response function for frequency dependent properties in solution: Application to polarizability and specific rotation. *J Chem Phys*. 2013;*139*(11):114103.
48. Caricato M, Lipparini F, Scalmani G, Cappelli C, Barone V. Vertical electronic excitations in solution with the EOM-CCSD method combined with a polarizable explicit/implicit solvent model. *J Chem Theory Comput*. 2013;*9*(7):3035–3042.
49. Caricato M. A comparison between state-specific and linear-response formalisms for the calculation of vertical electronic transition energy in solution with the CCSD-PCM method. *J Chem Phys*. 2013;*139*(4):044116.
50. Caricato M. A corrected-linear response formalism for the calculation of electronic excitation energies of solvated molecules with the CCSD-PCM method. *Comp Theor Chem*. 2014;*1040-1041*:99–105.
51. Ren S, Harms J, Caricato M. An EOM-CCSD-PCM benchmark for electronic excitation energies of solvated molecules. *J Chem Theory Comput*. 2017;*13*(1):117–124.
52. Caricato M. Linear response coupled cluster theory with the polarizable continuum model within the singles approximation for the solvent response. *J Chem Phys*. 2018;*148*:134113.
53. Ren S, Lipparini F, Mennucci B, Caricato M. Coupled cluster theory with induced dipole polarizable embedding for ground and excited states. *J Chem Theory Comput*. 2019;*15*(8):4485–4496.
54. Caricato M. CCSD-PCM excited state energy gradients with the linear response singles approximation to study the photochemistry of molecules in solution. *ChemPhotoChem*. 2019;*3*(0):747–754.
55. Scalmani G, Frisch MJ. Continuous surface charge polarizable continuum models of solvation. I. General formalism. *J Chem Phys*. 2010;*132*(11):114110.
56. Cossi M, Rega N, Scalmani G, Barone V. Energies, structures, and electronic properties of molecules in solution with the C-PCM solvation model. *J Comput Chem*. 2003;*24*(6):669–681.
57. Klamt A, Schüürmann G. COSMO: A new approach to dielectric screening in solvents with explicit expressions for the screening energy and its gradient. J Chem Soc. *Perkin Trans*. 1993;*2*(5):799–805.
58. Lipparini F, Scalmani G, Mennucci B, Cances E, Caricato M, Frisch MJ. A variational formulation of the polarizable continuum model. *J Chem Phys*. 2010;*133*(1):014106.
59. Ribeiro RF, Marenich AV, Cramer CJ, Truhlar DG. Use of solution-phase vibrational frequencies in continuum models for the free energy of solvation. *J Phys Chem B*. 2011;*115*(49):14556–14562.
60. Gauss J, Stanton JF, Bartlett RJ. Coupled-cluster open-shell analytic gradients: Implementation of the direct product decomposition approach in energy gradient calculations. *J Chem Phys*. 1991;*95*(4):2623–2638.
61. Salter EA, Trucks GW, Bartlett RJ. Analytic energy derivatives in many-body methods. 1. 1st derivatives. *J Chem Phys*. 1989;*90*(3):1752–1766.
62. Pople JA, Krishnan R, Schlegel HB, Binkley JS. Derivative studies in hartree-fock and møller-plesset theories. *Int J Quantum Chem*. 1979;*16*(S13):225–241.
63. Frisch MJ, Head-Gordon M, Pople JA. Direct analytic SCF 2nd derivatives and electric-field properties. *Chem Phys*. 1990;*141*(2–3):189–196.
64. Frisch MJ, Trucks GW, Schlegel HB, et al. *Gaussian 16 Revision C.01*. Wallingford, CT: Gaussian Inc., 2016.
65. Frisch MJ, Trucks GW, Schlegel HB, et al. *Gaussian DV: Rev I.09*. Wallingford, CT: Gaussian Inc., 2009.
66. Scalmani G, Frisch MJ, Mennucci B, Tomasi J, Cammi R, Barone V. Geometries and properties of excited states in the gas phase and in solution: Theory and application of a time-dependent density functional theory polarizable continuum model. *J Chem Phys*. 2006;*124*(9):094107.
67. Cammi R, Corni S, Mennucci B, Tomasi J. Electronic excitation energies of molecules in solution: State specific and linear response methods for nonequilibrium continuum solvation models. *J Chem Phys*. 2005;*122*(10):104513–104512.
68. Corni S, Cammi R, Mennucci B, Tomasi J. Electronic excitation energies of molecules in solution within continuum solvation models: Investigating the discrepancy between state-specific and linear-response methods. *J Chem Phys*. 2005;*123*(13):134512–134510.
69. Stanton JF, Bartlett RJ. The equation of motion coupled-cluster method. A systematic biorthogonal approach to molecular excitation energies, transition probabilities, and excited state properties. *J Chem Phys*. 1993;*98*(9):7029–7039.
70. Koch H, Jorgensen P. Coupled cluster response functions. *J Chem Phys*. 1990;*93*(5):3333–3344.
71. Koch H, Kobayashi R, de Merás AS, Jorgensen P. Calculation of size-intensive transition moments from the coupled cluster singles and doubles linear response function. *J Chem Phys*. 1994;*100*(6):4393–4400.
72. Caricato M, Trucks GW, Frisch MJ. On the difference between the transition properties calculated with linear response- and equation of motion-CCSD approaches. *J Chem Phys*. 2009;*131*(17):174104.
73. Kállay M, Gauss J. Calculation of excited-state properties using general coupled-cluster and configuration-interaction models. *J Chem Phys*. 2004;*121*(19):9257–9269.
74. Marenich AV, Cramer CJ, Truhlar DG, et al. Practical computation of electronic excitation in solution: Vertical excitation model. *Chem Sci*. 2011;*2*:2143–2161.
75. Barron LD. *Molecular light scattering and optical activity*. Cambridge: Cambridge University Press, 2004.
76. Crawford TD, Tam MC, Abrams ML. The current state of Ab initio calculations of optical rotation and electronic circular Dichroism spectra. *J Phys Chem A*. 2007;*111*(48):12057–12068.
77. Lipparini F, Barone V. Polarizable force fields and polarizable continuum model: A fluctuating charges/PCM approach. 1. Theory and implementation. *J Chem Theory Comput*. 2011;*7*(11):3711–3724.

78. Loco D, Polack É, Caprasecca S, et al. A QM/MM approach using the AMOEBA polarizable embedding: From ground state energies to electronic excitations. *J Chem Theory Comput*. 2016;*12*(8):3654–3661.
79. Wang J, Cieplak P, Li J, Hou T, Luo R, Duan Y. Development of polarizable models for molecular mechanical calculations I: Parameterization of atomic polarizability. *J Phys Chem B*. 2011;*115*(12):3091–3099.
80. Caprasecca S, Jurinovich S, Viani L, Curutchet C, Mennucci B. Geometry optimization in polarizable QM/MM models: The induced dipole formulation. *J Chem Theory Comput*. 2014;*10*(4):1588–1598.
81. Marenich AV, Cramer CJ, Truhlar DG. Universal solvation model based on solute electron density and on a continuum model of the solvent defined by the bulk dielectric constant and atomic surface tensions. *J Phys Chem B*. 2009;*113*(18):6378–6396.
82. Rappe AK, Casewit CJ, Colwell KS, Goddard WA, Skiff WM. UFF, a full periodic table force field for molecular mechanics and molecular dynamics simulations. *J Am Chem Soc*. 1992;*114*(25):10024–10035.
83. Caricato M, Trucks GW, Frisch MJ, Wiberg KB. Electronic transition energies: A study of the performance of a large range of single reference density functional and wave function methods on valence and Rydberg states compared to experiment. *J Chem Theory Comput*. 2010;*6*(2):370–383.
84. Crawford TD, Stephens PJ. Comparison of time-dependent density-functional theory and coupled cluster theory for the calculation of the optical rotations of chiral molecules. *J Phys Chem A*. 2008;*112*(6):1339–1345.
85. Aharon T, Lemler P, Vaccaro PH, Caricato M. Comparison of measured and predicted specific optical rotation in gas and solution phases: A test for the polarizable continuum model of solvation. *Chirality*. 2018;*30*:383–395.
86. Parusel ABJ, Köhler G, Nooijen M. A coupled-cluster analysis of the electronic excited states in Aminobenzonitriles. *J Phys Chem A*. 1999;*103*(20):4056–4064.
87. Köhn A, Hättig C. On the nature of the low-lying singlet states of 4-(dimethyl-amino)benzonitrile. *J Am Chem Soc*. 2004;*126*(23):7399–7410.
88. Wiggins P, Williams JAG, Tozer DJ. Excited state surfaces in density functional theory: A new twist on an old problem. *J Chem Phys*. 2009;*131*(9):091101.
89. Kochman MA, Tajti A, Morrison CA, Miller RJD. Early events in the nonadiabatic relaxation dynamics of 4-(N,N-Dimethylamino)benzonitrile. *J Chem Theory Comput*. 2015;*11*(3):1118–1128.
90. Lunkenheimer B, Köhn A. Solvent effects on electronically excited states using the conductor-like screening model and the second-order correlated method ADC(2). *J Chem Theory Comput*. 2013;*9*(2):977–994.
91. Curchod BFE, Sisto A, Martínez TJ. Ab initio multiple spawning photochemical dynamics of DMABN using GPUs. *J Phys Chem A*. 2017;*121*(1):265–276.
92. Georgieva I, Aquino AJA, Plasser F, Trendafilova N, Köhn A, Lischka H. Intramolecular charge-transfer excited-state processes in 4-(N,N-Dimethylamino)benzonitrile: The role of twisting and the $\pi\sigma^*$ state. *J Phys Chem A*. 2015;*119*(24):6232–6243.
93. Mewes JM, Herbert JM, Dreuw A. On the accuracy of the general, state-specific polarizable-continuum model for the description of correlated ground and excited states in solution. *Phys Chem Chem Phys*. 2017;*19*(2):1644–1654.
94. Schwabe T. General theory for environmental effects on (vertical) electronic excitation energies. *J Chem Phys*. 2016;*145*(15):154105.
95. Duchemin I, Guido CA, Jacquemin D, Blase X. The Bethe-Salpeter formalism with polarisable continuum embedding: Reconciling linear-response and state-specific features. *Chem Sci*. 2018;*9*(19):4430–4443.

How to cite this article: Caricato M. Coupled cluster theory in the condensed phase within the singles-T density scheme for the environment response. *WIREs Comput Mol Sci*. 2020;e1463. https://doi.org/10.1002/wcms.1463